國 立 交 通 大 學

電子工程學系 電子研究所碩士班

碩 士 論 文

在負偏壓溫度不穩定回復時臨界電壓改變量分佈之統計特性和模式及其時間演繹

Statistical Characterization and Modeling of ΔV_{th} Distribution in NBTI Recovery and Its Time Evolution

研 究 生 ：謝泓達

指導教授 ：汪大暉 博士

中華民國 一〇一 年 七 月

在負偏壓溫度不穩定回復時臨界電壓改變量分佈之統計特性和模式及其時間演繹

Statistical Characterization and Modeling of ΔV_{th} Distribution in NBTI Recovery and Its Time Evolution

研 究 生 ： 謝泓達　　Student : Hung-Da, Hsieh

指導教授 ： 汪大暉 博士　　Advisor : Dr. Tahui Wang

國立交通大學

電子工程學系 電子研究所碩士班

碩士論文

A Thesis

Submitted to Department of Electronics Engineering and
Institute of Electronics
College of Electrical and Computer Engineering
National Chiao Tung University
in Partial Fulfillment of the Requirements
for the Degree of
Master of Science
in
Electronic Engineering

July 2012
Hsinchu, Taiwan, Republic of China.

中華民國 一〇一 年 七 月

在負偏壓溫度不穩定回復時臨界電壓改變量分佈之統計特性和模式及其時間演繹

學生：謝泓達　　指導教授：汪大暉 博士

國立交通大學　電子工程學系　電子研究所

摘要

在本篇論文中，為了了解負偏壓溫度回復時的臨界電壓改變量分佈特性，我們萃取單一電荷散逸導致臨界電壓改變量，還有單一電荷散逸時間。

我們考慮了活化能(Activation Energy)和缺陷能量(Trap Energy)分佈來模擬負偏壓溫度(NBT)操作後的回復(Recovery)效應之散逸時間(De-trapping Time)散佈。此外，也研究在經過負偏壓溫度操作後回復時，單一電荷散逸導致臨界電壓改變量的散佈。我們把這兩個散佈結合到電荷散逸模型(Trapped Charge Emission Model)。由上述兩個實驗參數來進行蒙地卡羅模擬經過負偏壓溫度操作後回復的臨界電壓散佈，此結果可精準符合實驗數據。

Statistical Characterization and Modeling of ΔV_{th} Distribution in NBTI Recovery and Its Time Evolution

Student: Hung-Da Hsieh Advisor: Dr. Tahui Wang

Department of Electronics Engineering &

Institute of Electronics

National Chiao Tung University

Abstract

In this thesis, single charge de-trapping induced threshold voltage shift (Δv_{th}) and single charge de-trapping time (τ_e) are extracted to analyze the characteristic of the threshold voltage (ΔV_{th}) dispersion in NBTI recovery.

Activation energy (E_a) and trap energy (E_T) distributions are investigated to simulate de-trapping time (τ_e) dispersion during negative bias temperature instability (NBTI) recovery. Furthermore, single charge de-trapping induced Δv_{th} dispersion is investigated during NBTI recovery. A statistical model combining the trapped charge emission model with the two dispersions is developed. According to the

characterization of the single charge phenomenon, we proposed a Monte Carlo simulation to simulate the NBTI recovery threshold voltage dispersion. Our model can fit the measured ΔV_{th} dispersion during NBTI recovery very well.

Acknowledgement

本篇論文之所以能夠完成，首先，我要感謝我的指導教授 — 汪大暉教授，在他嚴謹紮實且耐心研究指導下，使我從中學習到新的知識及正確的研究態度，在此深表我對老師的感謝。

另外，博士班學長 — 小馬學長、榮標學長、岳庭學長、佑亮學長，碩士班學長 — 志宇學長、明瑋學長、書祥學長，帶領我融入實驗室，並且教導我量測技術和實驗原理，尤其是榮標學長，兩年來無私的指導，每當遇到困難時，常常幫我解決當下難題，使我受益良多。再來要感謝實驗室同學 — 定樺、英傑、政達、漢旻、侑璉的陪伴，讓我兩年的研究生生活充滿樂趣。

最後就是要感謝我的父母、家人以及女朋友，有了他們的鼓勵，讓我在感到疲倦的時候有繼續往下走的動力，讓我完成碩士學位。

2012.7

Contents

Chinese Abstract *i*

English Abstract *ii*

Acknowledgement *iv*

Contents *v*

Figure Captions *vi*

Chapter 1 Introduction *1*

Chapter 2 Single Charge Effect in NBTI Recovery *5*

2.1 Preface *5*

2.2 Device Details and Measurement Setup *5*

2.3 Δv_{th} Probability Distribution in NBTI Recovery *6*

2.4 Single Charge De-trapping Time Distribution *7*

2.5 ΔV_{th} versus Number of De-trapping Hole in NBTI Recovery *7*

Chapter 3 Physical Origins of ΔV_{th} Distribution during NBTI Recovery *20*

3.1 Preface *20*

3.2 Extraction E_a from $\tau_{e,i}$ Distributions *20*

3.3 Monte Carlo Simulation of ΔV_{th} Distribution *22*

3.4 Closed Form Derivation *23*

Chapter 4 Conclusion *42.*

Reference *43*

Figure Captions

Chapter 1

Fig. 1.1 NBTI/PBTI induced V_{th} drift versus stress time in high-κ/metal gate MOSFETs. *3.*

Fig. 1.2 Recovery data after three selected stress times obtained at different stress voltages. *4.*

Chapter 2

Fig. 2.1 In this thesis, we characterize NBTI recovery in high-κ/metal gate pMOSFETs with gate length of 30nm and gate width of 80nm. *9.*

Fig. 2.2 The instrument setting is used for the fast transient measurement. *10.*

Fig. 2.3 (a) Waveforms applied to gate and drain during stress and measurement. *11.*

(b) Schematic illustration of holes de-trapping formation during NBTI recovery.

Fig. 2.4 We can extract Δv_{th} and τ_e from the stair-like threshold voltage trace in NBTI recovery. *12.*

Fig. 2.5 Complementary cumulative probability distribution of single de-trapping hole induced Δv_{th} in NBTI recovery. *13.*

Fig. 2.6 When the trapped charge locates on the main current path, it will induce larger Δv_{th} amplitude. *14.*

Fig. 2.7 Individual threshold voltage shift is a stair-like trace. The average threshold voltage shift has logarithmic time dependent in NBTI recovery. *15.*

Fig. 2.8 The first three individual de-trapping time (τ_e) probability distribution are Gaussian-like distribution. *16.*

Fig. 2.9 The occurrence of total τ_e distribution is uniform. *17.*

Fig. 2.10 ΔV_{th} versus Number of De-trapping Hole *18*

Table I μ_i and σ_i of the first three de-trapping time distribution. *19.*

Chapter 3

Fig. 3.1 Schematic representation of band diagram and trap positions in recovery phase. *27.*

Fig. 3.2 Flow of E_a extraction *28.*

Fig. 3.3 Extracted E_a from $\tau_{e,i}$ Distribution *29.*

Fig. 3.4 Flow chart of Monte Carlo simulation. *30.*

Fig. 3.5 The probability distribution of trapped charge de-trapping time (τ_e) in NBTI recovery. Monte Carlo simulation result fits the measurement data well. *31.*

Fig. 3.6 MC simulation result of total τ_e distribution. *32.*

Fig. 3.7 Simulation of stair-like ΔV_{th} fluctuation. *33.*

Fig. 3.8 Probability distribution of NBTI recovery induced ΔV_{th} at 0.1s, 10s, and 1000s from measurement and Monte Carlo simulation. *34.*

Fig. 3.9 The mean value of the ΔV_{th} distribution versus NBTI recovery time from measurement and Monte Carlo simulation. Percolation has δ-function like E_a and E_T distribution. *35.*

Fig. 3.10 The variance of the ΔV_{th} distribution versus NBTI recovery time from measurement and Monte Carlo simulation. Percolation has δ-function like E_a and E_T distribution. *36.*

Fig. 3.11 Flow chart of closed form method. *37.*

Fig. 3.12 The (a) mean value and (b) variance of the ΔV_{th} distribution versus NBTI recovery time from Monte Carlo simulation and closed form method. *38.*

Table II σ of extracted E_a from $\tau_{e,1}$, $\tau_{e,2}$, and $\tau_{e,3}$. *39.*

Table III μ and σ of the first three de-trapping time distribution from measurement and Monte Carlo simulation. *40.*

Table IV μ, σ^2, and probability of each de-trapping hole number. *41.*

Chapter 1
Introduction

For downscaling metal-oxide-semiconductor field-effect-transistor (MOSFET) devices, thickness of gate dielectric is required to be smaller in the progressive technology node. Below the physical thickness of 16 Å, the gate leakage current exceeds the specifications (1 A/cm) [1]. Recently, the high permittivity (high-κ) dielectrics have been proposed to solve this problem due to its higher physical thickness while keeping the same EOT [2]. Although significant reductions in the gate leakage have been achieved, two major issues remain for CMOS circuit applications: 1) the high threshold voltages [3] and 2) polysilicon (poly-Si) depletion. Consequently, sub-45nm CMOS technology scaling will likely utilize high-κ/metal gate stacks. And the SiO_2 interfacial layer offers better device performance and quality of the oxide/Si interface than high-κ dielectrics directly placed on the Si substrate.

A high-κ/metal gate stack is required for scaled MOSFETs, but one of its most serious problems is in V_{th} control. The BTI degradation of high-κ/metal gate devices can be seen to be much more severe. NBTI is nowadays the most critical device degradation mechanism and became a limiting factor in scaling of modern CMOS technologies (Fig.1.1) [4]. PMOS Negative Bias Temperature Instability (NBTI) degrades threshold voltage and drive current, raising an important concern for analog and digital circuits. However, NBTI recovery is an important consideration particularly for typical CMOS operation where applied gate bias switches between "high" and "low" voltages repeatedly [5]. Trapped charge would emit when the

applied gate bias is “low” voltage which is known as the recovery mode. The NBTI recovery phenomenon leads to a fast reduction of the stress induced electrical device parameter degradation after end of stress. The NBTI recovery phenomenon endangers proper lifetime estimation. In the past, many experimental and theoretical attempts have been made in order to explain the logarithm time dependence of V_{th} recovery over many decades of time (Fig. 1.2). From these studies, two main NBTI mechanisms have emerged **[6]-[9]**.

In Chapter 2, stair-like drain current traces are observed in the small size devices during NBTI Recovery **[10]-[12]**. In the recovery phase, the tapped charges emit from the high-k layer by thermal assisted tunneling. Single charge de-trapping induced Δv_{th} amplitude and its de-trapping time are extracted from the measurement data.

In Chapter 3, it is found that the de-trapping time ($\tau_{e,i}$) distributions are Gaussian-like distributions. E_a distribution can be extracted from the de-trapping time distributions. We assume that the trap energy distribution is uniform. Based on the distributions of E_a and E_T, we simulate the de-trapping time distributions. The de-trapping time distributions are related to the fluctuation of de-trapping hole number. According to the probability distribution of Δv_{th}, each single charge de-trapping induced Δv_{th} amplitude is simulated. Consequently, staircase-like ΔV_{th} trace during NBTI recovery can be demonstrated a by Monte Carlo simulation. The mean and variance of ΔV_{th} are acquired during NBTI recovery. We also derive the ΔV_{th} distribution by closed form method. Finally, we give a conclusion in Chapter 4.

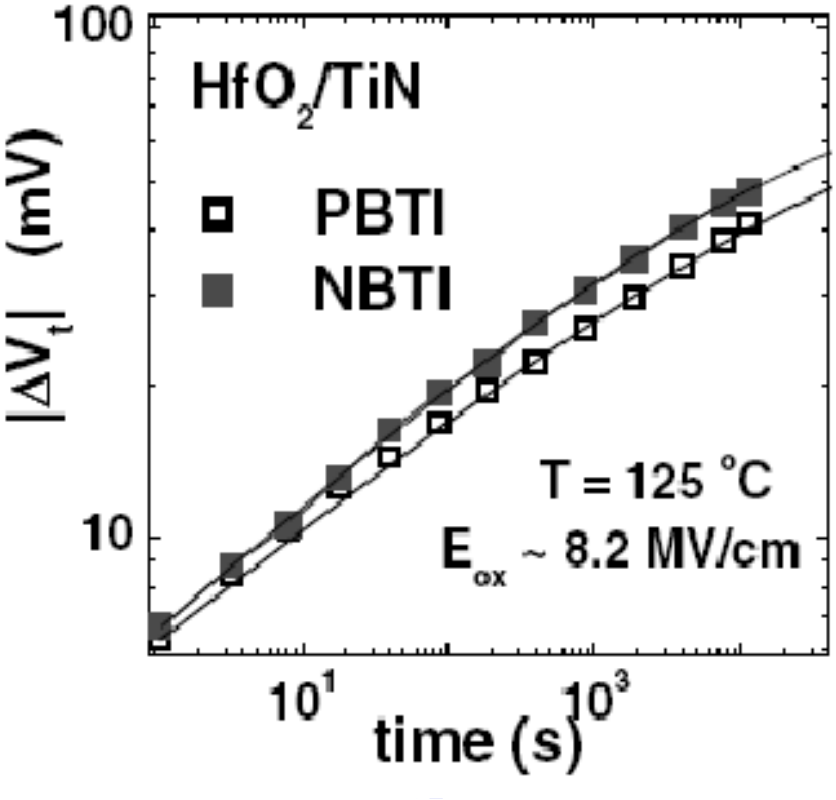

Fig. 1.1 NBTI/PBTI induced V_{th} drift versus stress time in high-κ/metal gate MOSFETs **[4]**.

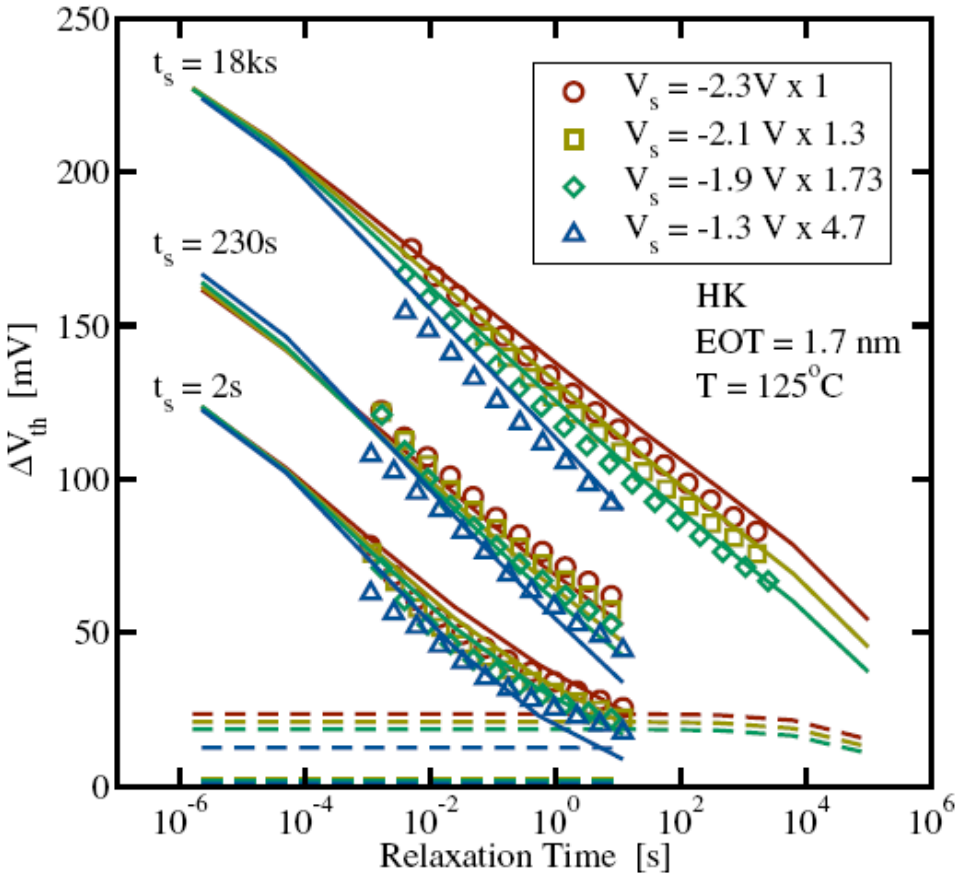

Fig. 1.2 Recovery data after three selected stress times obtained at different stress voltages **[16]**.

Chapter 2
Single Charge Effect in NBTI Recovery

2.1 Preface

It is commonly accepted that mechanism of BTI is due to charge trapping in the high-κ layer **[13]**. BTI is characterized by stressing transistor at high temperature and electric field, periodically interrupting the stress to monitor threshold voltage or drain current ("SMS" technique). The other way to investigate BTI effect is to measure post-stress recovery behavior **[14]**.

To identify the charge de-trapping mechanism, a direct measurement of single charge effect is demonstrated, in which the stair-like threshold voltage trace is measured. The Δv_{th} probability distribution is found by extracting the threshold voltage amplitude caused by single charge emission. We also extract single charge de-trapping time, and it is found that the first three individual de-trapping time distribution are Gaussian-like distributions. The occurrence of total de-trapping time distribution is a uniform distribution. According to the tunneling front model, this implies the trap is a uniform distribution in high-κ layer spatially.

2.2 Device Details and Measurement setup

The device structure we used in this thesis is illustrated in Fig. 2.1. The devices are pMOSFETs with a metal gate (TiN) and a bi-layer gate dielectric stack consisting of HfON and interfacial SiON layer (IL). The gate length and width are 30nm and 80nm respectively. Its equivalent oxide thickness (EOT) is 7.8 Å .

The Measurement setup is shown in Fig. 2.2. A two channel Agilent B1500 pulse generator connects to drain and gate electrode and it changes the gate bias and drain bias simultaneously. The pulse waveform is shown in Fig. 2.3(a). First, we measure the devices initial state to extract fresh V_{th} @I_d=500nA. Then, the devices are subjected to a negative gate bias (Vg=-1.8V) stress during 100s, and recover at fresh V_{th} during 1000s. In the recovery phase, the trapping holes will emit by thermally assisted tunneling (TAT), as shown in Fig. 2.3(b).

2.3 Δv_{th} Probability Distribution in NBTI Recovery

The recovery ΔV_{th} exhibits a stair-like trace, as shown in Fig. 2.4. Each jump in Fig. 2.4 is believed due to a single trapped hole emission from the high-κ layer. The Δv_{th} amplitude is extracted, as shown in Fig. 2.4. The probability distribution of Δv_{th} amplitude exhibits an exponential function.

$$f\left(\Delta v_{th}\right)=\frac{1}{\sigma}\exp\left(-\frac{\Delta v_{th}}{\sigma}\right) \qquad \text{Eq. (2.1)}$$

The cumulative probability distribution, as illustrated in Fig. 2.5, can be expressed below,

$$f\left(\Delta v_{th}\right)=\exp\left(-\frac{\Delta v_{th}}{\sigma}\right) \qquad \text{Eq. (2.2)}$$

The Δv_{th} distribution is attributed to a current path percolation effect due to random dopants in substrate (Fig. 2.6) **[15]**. According to the Eq. (2.2), the slope of the distribution is -1/σ, as shown in Fig. 2.5. The physical meaning of σ is the average Δv_{th} induced by single charge de-trapping. Average of each stair-like ΔV_{th} trace is

shown in Fig. 2.7. The ΔV_{th} versus recovery time follows logarithmic dependence **[8], [16]**. This phenomenon is observed in bigger-size devices.

2.4 Single Charge De-trapping Time Distribution

We measure the emission times of the first de-trapping hole (τ_{e1}), the second de-trapping hole (τ_{e2}) and the third de-trapping hole (τ_{e3}), respectively (Fig. 2.4). The first three individual de-trapping time distributions ($\tau_{e1,}$ $\tau_{e2,}$ *and* τ_{e3}) are shown in Fig. 2.8. It is found that each de-trapping time distribution is a Gaussian-like distribution and their μ_i and σ_i are shown in Table I.

$$f(\log(\tau_{e,i})) = \frac{1}{\sqrt{2\pi}\sigma_i}\exp[\frac{-(\log(\tau_{e,i}) - \mu_i)^2}{2\sigma_i^2}] \qquad \text{Eq. (2.3)}$$

The de-trapping time ($\tau_{e,\,i}$) distribution broadens with an increasing the index i. The occurrence of total τ_e distribution, as shown in Fig. 2.9, is a uniform distribution. According to the tunneling front model, the traps in the high-κ are uniform distribution in gate-to-substrate direction.

$$\tau_e \propto \exp(\alpha x) \qquad \text{Eq. (2.4)}$$

2.5 ΔV_{th} versus Number of De-trapping Hole in NBTI Recovery

ΔV_{th} distribution is measured at different recovery times. The total ΔV_{th} and number of de-trapping hole is extracted. The measurement results at the recovery time

of 0.1(s), 10(s), and 1000(s) are shown in Fig. 2.10. Each data point represents a device. The slope of straight line is the average of single hole de-trapping induced ΔV_{th}. As shown in Fig. 2.10., distributions of the de-trapping hole number and ΔV_{th} broaden with an increasing recovery time.

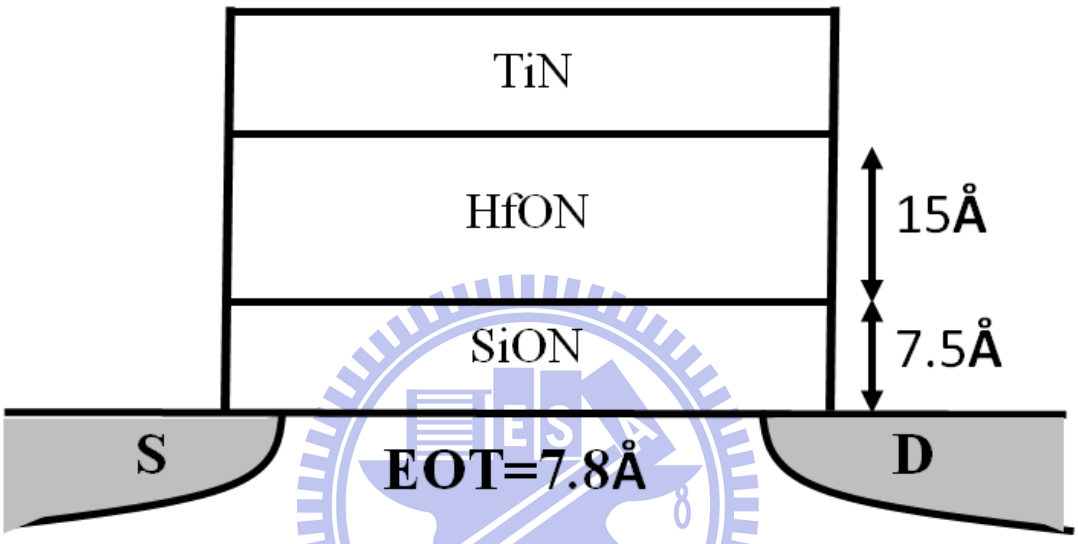

Fig. 2.1 In this thesis, we characterize NBTI recovery in high-κ/metal gate pMOSFETs with gate length of 30nm and gate width of 80nm.

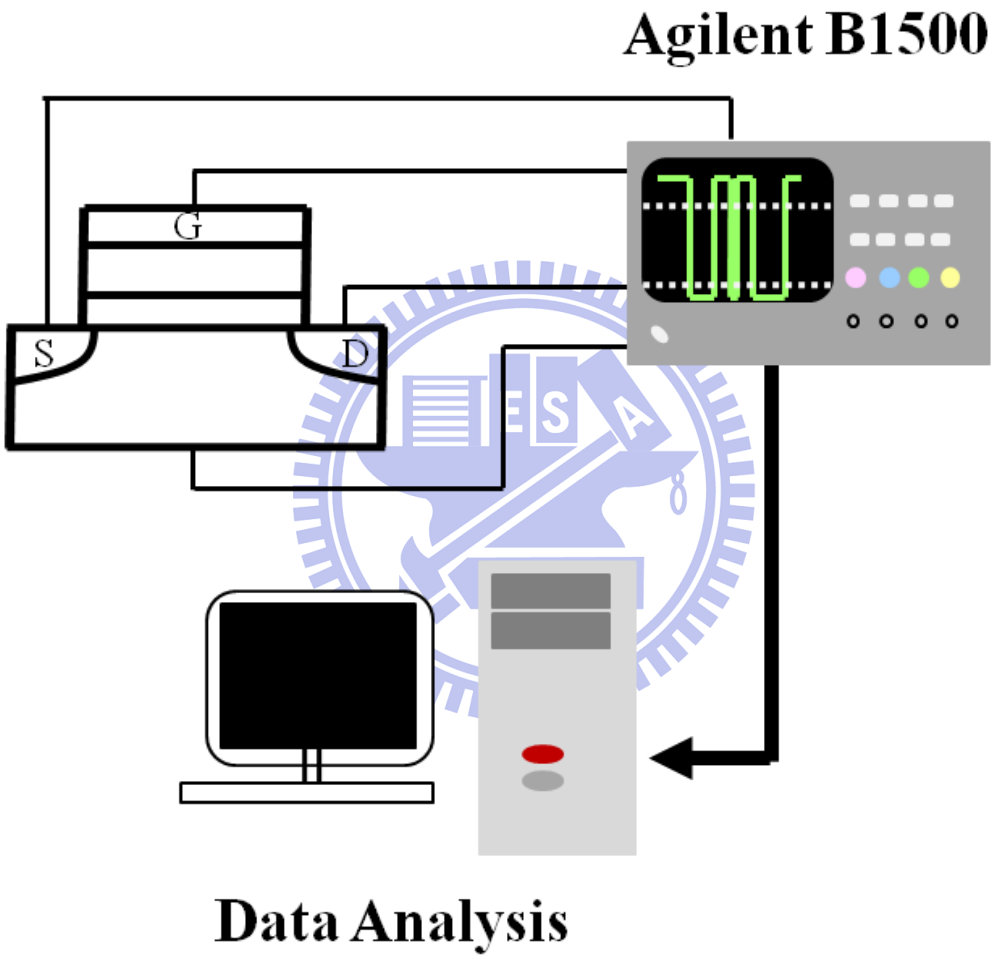

Fig. 2.2 The instrument setting is used for the fast transient measurement.

(a)

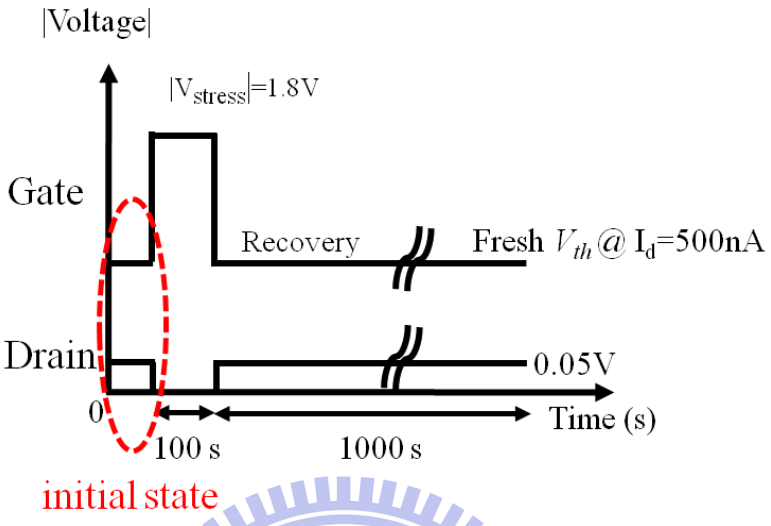

(b)

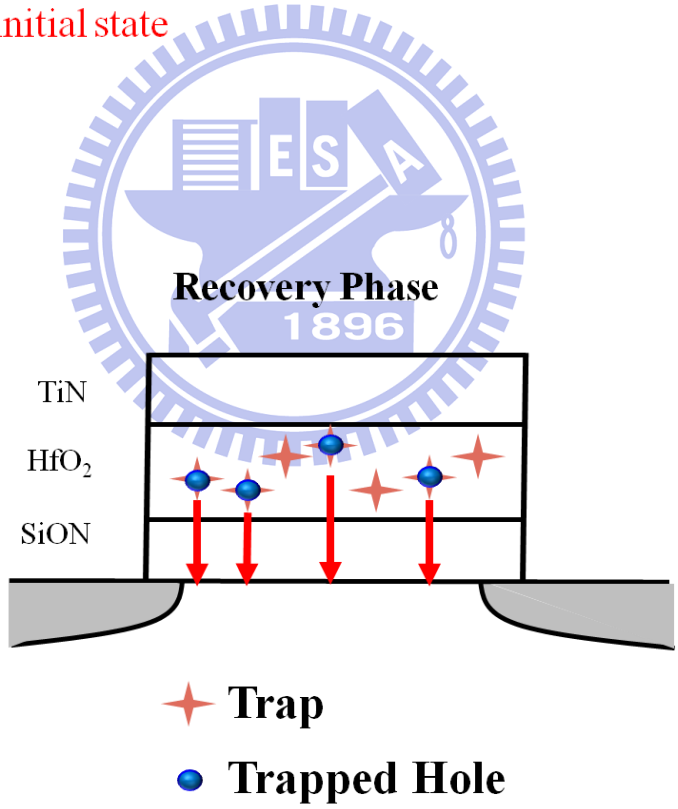

Fig. 2.3 (a) Waveforms applied to gate and drain during stress and measurement. (b) Schematic illustration of hole de-trapping formation during NBTI recovery.

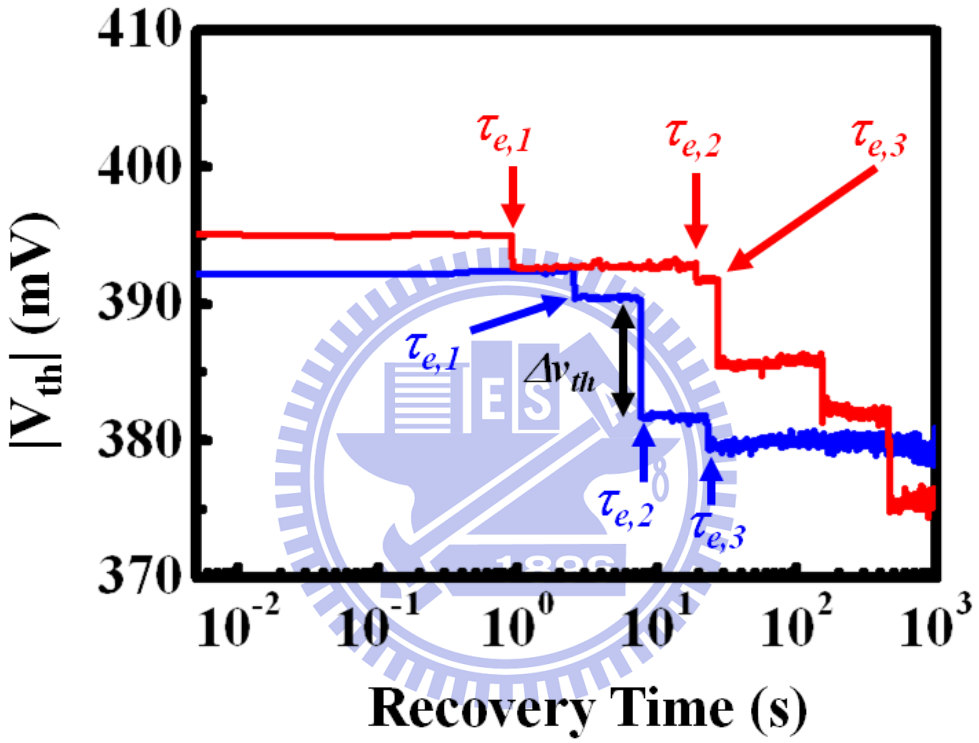

Fig. 2.4 We can extract Δv_{th} and τ_e from the stair-like threshold voltage trace in NBTI recovery.

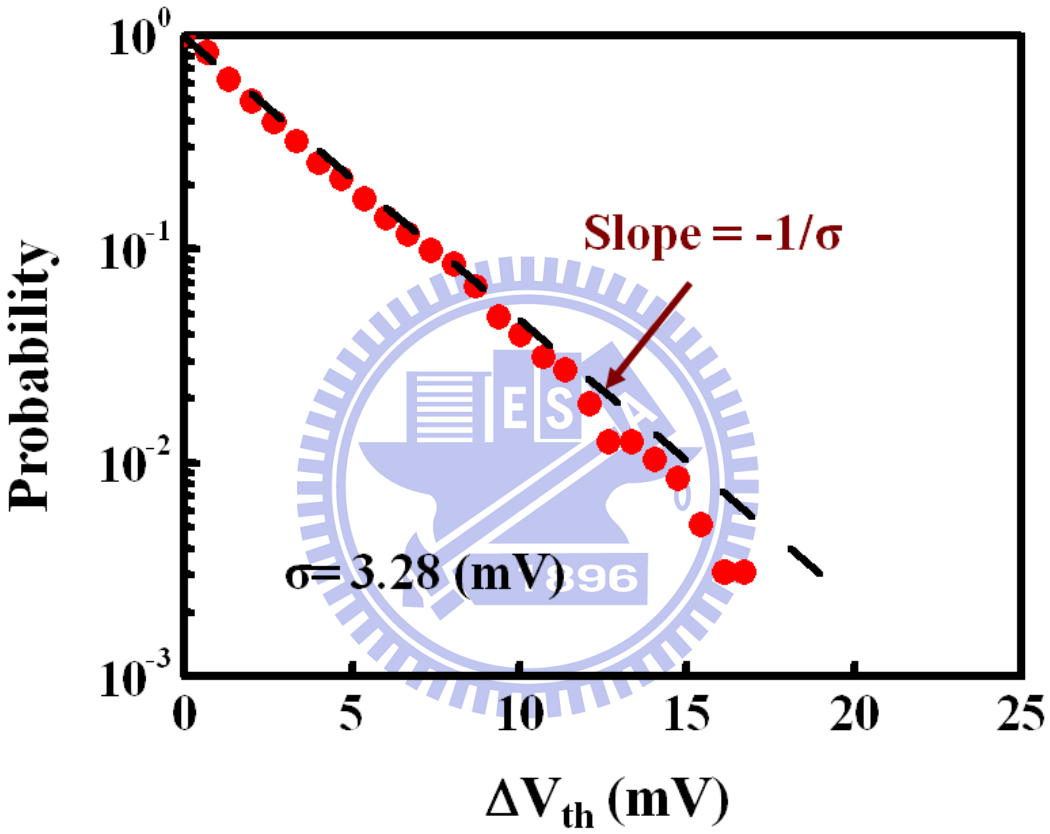

Fig. 2.5 Complementary cumulative probability distribution of single de-trapping hole induced Δv_{th} in NBTI recovery.

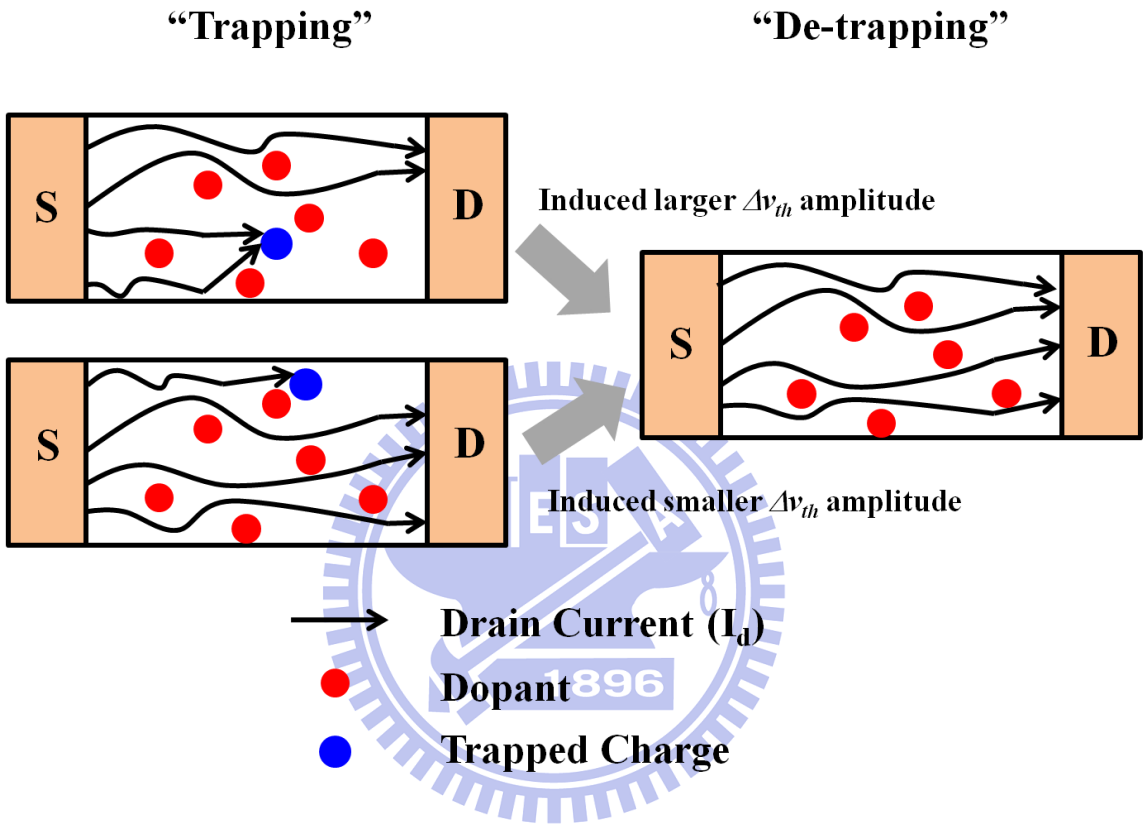

Fig. 2.6 When the trapped charge locates on the main current path, it will induce larger Δv_{th} amplitude.

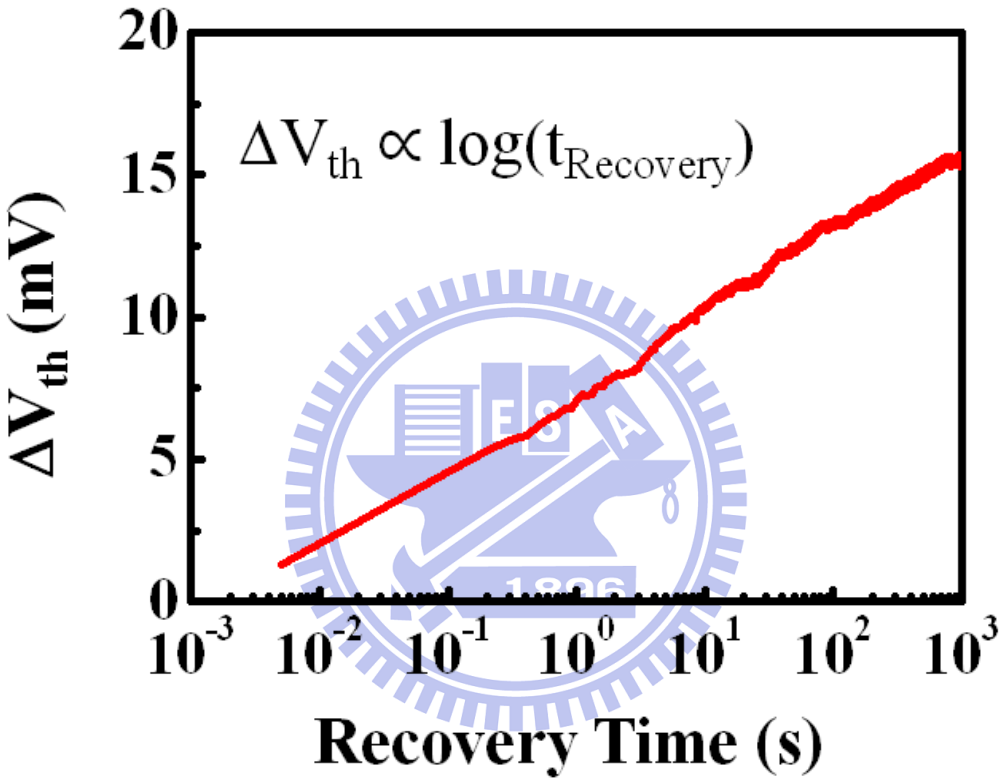

Fig. 2.7 Individual threshold voltage shift is a stair-like trace. The average threshold voltage shift has logarithmic time dependent in NBTI recovery.

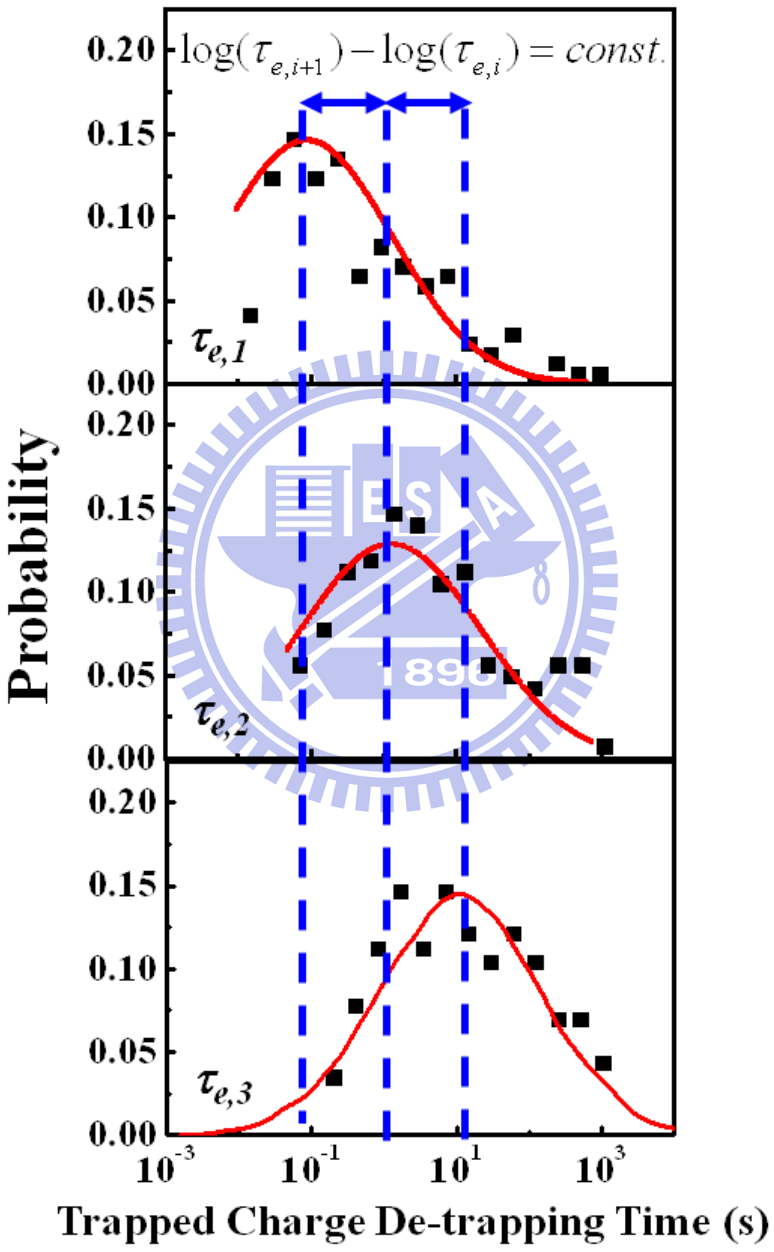

Fig. 2.8 The first three individual de-trapping (τ_e) probability distribution are Gaussian-like distribution.

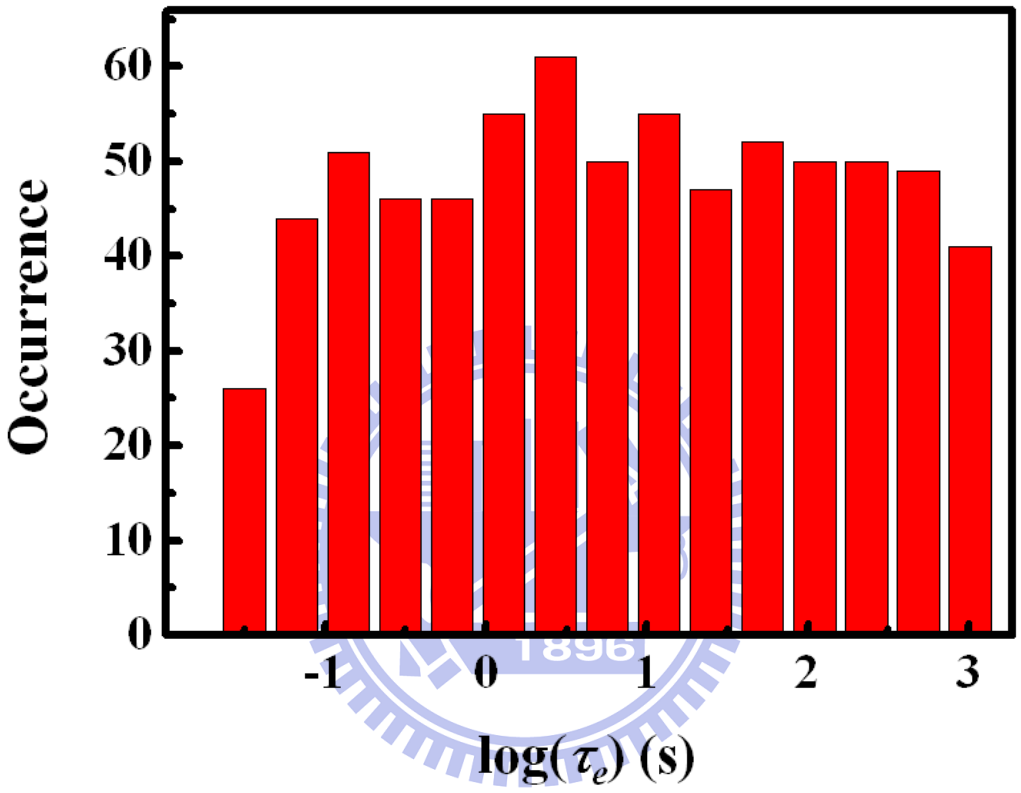

Fig. 2.9 The occurrence of total τ_e distribution is uniform.

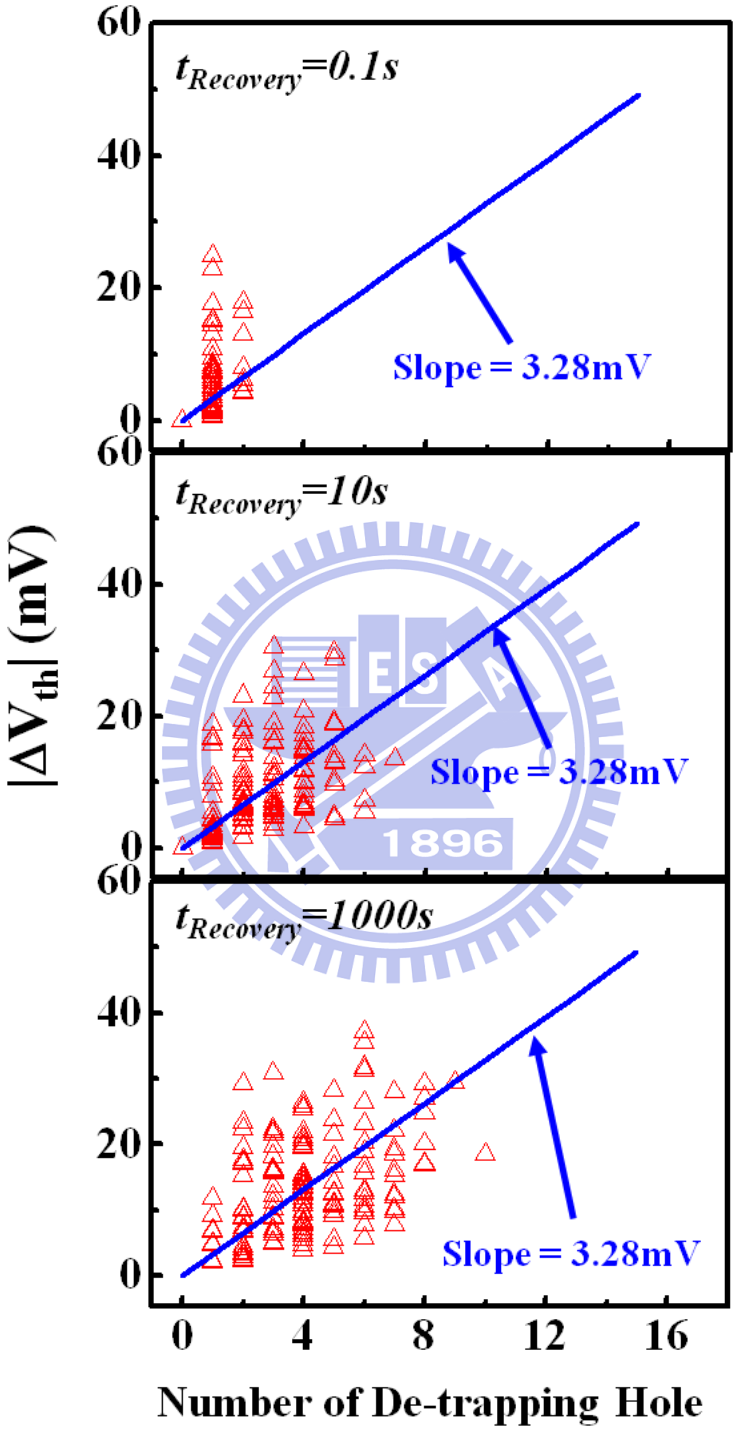

Fig. 2.10 ΔV_{th} versus Number of De-trapping Hole

i	1	2	3
μ_i	-1.019	0.036	1.064
σ_i	1.070	1.181	1.285

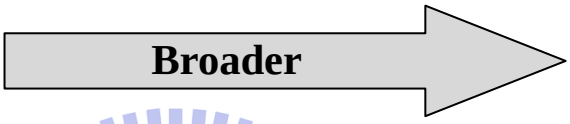

Table I μ_i and σ_i of the first three de-trapping time distribution

Chapter 3
Simulation of ΔV_{th} Dispersion during NBTI Recovery

3.1 Preface

Physical origins of ΔV_{th} distribution during NBTI recovery in pMOSFETs are explored and characterized. Two factors are found to affect a NBTI ΔV_{th} distribution. One is the dispersion of single charge de-trapping induced Δv_{th}. The other one is the dispersion of de-trapping time. In the previous chapter, it is found that the first three individual de-trapping time distributions are Gaussian-like distributions. We attribute de-trapping time distribution to activation energy (E_a) and trap energy (E_T) distribution in the trapped charge emission model **[10]**. A statistical model combining the trapped charge emission model with the two dispersions is developed. Our simulation result fits the measured ΔV_{th} dispersion during NBTI recovery very well. Furthermore, we derive the ΔV_{th} dispersion using closed form method, and its result fit the measured data very well.

3.2 Extraction E_a from $\tau_{e,i}$ Distributions

Single charge phenomenon is measured in the previous chapter. The individual de-trapping time distribution is a Gaussian-like distribution. From the measured $\tau_{e,i}$ distributions, E_a is extracted using trapped charge emission model. The formula of trapped charge emission model is expressed below,

$$\tau_{e,i} = \tau_0 \exp(\frac{E_a}{kT}) \exp(\alpha_{IL} T_{IL}) \exp(\alpha_k x_i) \qquad \text{Eq. (3.1)}$$

where

$$\tau_0 = [N_v(1-f_v)\sigma V_{th}]^{-1} \qquad \text{Eq. (3.1-a)}$$

$$\alpha_{IL} = \frac{2\sqrt{2m_{IL}^{*}q(E_T+\phi_B)}}{\hbar} \quad ; \quad \alpha_k = \frac{2\sqrt{2m_k^{*}qE_T}}{\hbar} \qquad \text{Eq. (3.1-b)}$$

m_{IL}*=0.41m_0 **[17]** ; m_k* =0.18m_0 **[18]**

Eq. (3.1) reveals the nature of tunneling for trapped hole emission time, $\tau_{e,i}$. N_v is the effective density-of-state in the Si valence band, and $N_v(1-f_v)$ is the amount of available states in Si substrate for out-tunneling holes from high-k traps. σ_0 represents the trap cross-section. Other variables have their usual definitions **[10]**. Energy band diagram is shown in Fig. 3.1. Our estimation is that the trap energy range is about 0.8eV by a 1-D Poisson simulation. E_T ranges between 0 and 0.8 eV from the Si valence band. In the formula definition, E_T ranges between 2.7 and 3.5 eV in our devices.

The flow of E_a extraction is shown in Fig. 3.2. First, we generate $\tau_{e,i}$ from the measurement data randomly, and we also generate x_i randomly. E_T is generated by a uniform distribution. As a result, E_a distributions can be calculated, as shown in Fig. 3.3. These E_a distributions are almost the same, and its standard deviation of E_a ($\sigma(E_a)$) is shown in Table II. The extracted E_a distributions are Gaussian-like distributions.

3.3 Monte Carlo Simulation of ΔV_{th} Distribution

A Monte Carlo simulation employing the trapped charge emission model and taking account the E_a and E_T distributions is developed to simulate a ΔV_{th} distribution and its recovery time evolution. Simulation flow is shown in Fig. 3.4. First, we assume E_T is a uniform distribution, and Ea is extracted from $\tau_{e,i}$ distributions. A statistical model combining the trapped charge emission model with the E_a and E_T distribution is developed. For reproducing the de-trapping time distribution, we would calculate its average (peak) value first. As illustrated in Fig. 2.8, the trap is a uniform distribution in gate-to-substrate direction. μ_i of each de-trapping time distribution is shown in Table I. It is found that $\mu_{i+1} - \mu_i$ equal about 1. The mean value of E_T ($\mu(E_T)$) equals to 3.1eV. As expressed in Eq. (3.2), we can get the $(x_{i+1}-\Delta x_i)$. Its value is about 3Å .

$$\log(\tau_{i+1}/\tau_i) = \frac{1}{\ln(10)} \frac{2\sqrt{2m_k^* q}}{\hbar} \cdot \sqrt{E_T}\,(x_{i+1} - x_i) \qquad \text{Eq. (3.2)}$$

MC simulation result is illustrated in Fig. 3.5. Its value is shown in Table III. Simulation result of total τ_e distribution is shown in Fig. 3.6. They all fit the experimental data well.

In our Monte Carlo simulation, an E_a is randomly selected according to extracted E_a and E_T according to a uniform distribution. The single hole de-trapping induced Δv_{th} dispersion and its de-trapping time distribution are characterized. Consequently, we can demonstrate the stair-like ΔV_{th} trace during NBTI recovery by MC simulation, as shown in Fig. 3.7. The slope of the dash line corresponds to an average ΔV_{th} caused

by a trapped hole emission. Fig. 3.8 shows probability distribution of NBTI recovery induced ΔV_{th} at 0.1s, 10s, and 1000s from measurement and Monte Carlo simulation. The ΔV_{th} distribution broadens with an increasing recovery time. The simulation results fit the measurement date well, especially in distribution tail. We extract the mean value and the variance of the ΔV_{th} distribution at different recovery times. The mean value of the ΔV_{th} follows a logarithm dependence on recovery time in five decades (Fig. 3.9). The variance of the ΔV_{th} distribution also increases with recovery time (Fig. 3.10). We can't simulate the ΔV_{th} distribution and its recovery time evolution exactly when we use the fixed E_a and E_T (Percolation Effect). Taking account the E_a and E_T distributions is essential to character the ΔV_{th} distribution during NBTI recovery.

3.4 Closed Form Derivation

In this section, we use another method to derive the ΔV_{th} distribution during NBTI recovery. Flow chart is shown in Fig. 3.11. E_a is a Gaussian distribution with μ=0.2(eV) and σ=0.08(eV). The probability of E_a is expressed below,

$$f(E_a) = \frac{1}{\sqrt{2\pi}\sigma} \exp[\frac{-(E_a - \mu)^2}{2\sigma^2}] \qquad \text{Eq. (3.4)}$$

E_T is a uniform distribution, and it ranges between 2.7 and 3.5 (eV).

$$f(E_T) = const. \qquad \text{Eq. (3.5)}$$

Taking the probability of E_a and E_T into Eq. (3.6), we can get the probability distribution of individual de-trapping time ($\tau_{e,m}$).

$$\tau_{e,m}(E_a, E_T, x_m) = \tau_0 \exp(\frac{E_a}{kT}) \exp(\alpha_{IL} T_{IL}) \exp(\alpha_k x_m) \quad \text{Eq. (3.6)}$$

With the SRH model, as expressed in Eq. (3.7), we derive the probability distribution of individual de-trapping time (τ_m*).

$$f(\tau_{e,m}) = \frac{1}{\tau_{e,m}} \exp(-\frac{\tau_m^*}{\tau_{e,m}}) \quad \text{Eq. (3.7)}$$

Then, we would calculate the de-trapping probability of each τ_m* at different recovery time. $P(A_m)$ stands for de-trapping probability of m-th de-trapping hole at a certain recovery time(t).

$$P(A_m) = \int_{-\infty}^{t} f(\tau_m^*)\, d\tau^* \quad \text{Eq. (3.8)}$$

$P(B_m)$ stands for the absence of the m-th de-trapping hole, can be expressed below,

$$P(B_m) = 1 - P(A_m) \quad \text{Eq. (3.9)}$$

The probability of total amount of m de-trapping holes at a recovery time (t) can be expressed below,

$$P(Num. = 0) = P_0 = \mathrm{P}(\mathrm{B}_1) * \mathrm{P}(\mathrm{B}_2) * \mathrm{P}(\mathrm{B}_3) * \ldots * \mathrm{P}(\mathrm{B}_n) = P(\bigcap_{m=1}^{M} B_m) \quad \text{Eq. (3.10)}$$

$$P(Num.=1)=P_1=P(A1)*P(B2)*P(B3)*\cdots+P(B1)*P(A2)*P(B3)*\cdots+\cdots$$
$$=\sum_{i=1}^{M}\frac{P(\bigcap_{m=1}^{M}B_m)}{P(B_i)}*P(A_i) \qquad \text{Eq. (3.11)}$$

$$P(Num.=2)=P_2=\sum_{\substack{i,j=1\\(j>i)}}^{M}\frac{P(\bigcap_{m=1}^{M}B_m)}{P(B_i)P(B_j)}*P(A_i)P(A_j) \qquad \text{Eq. (3.12)}$$

$$P(Num.=3)=P_3=\sum_{\substack{i,j,k=1\\(k>j>i)}}^{M}\frac{P(\bigcap_{m=1}^{M}B_m)}{P(B_i)P(B_j)P(B_k)}*P(A_i)P(A_j)P(A_k) \qquad \text{Eq. (3.13)}$$

And so on.

M is the maximum de-trapping number of our measured devices.

As aforementioned, the trap number distribution is calculated and its average and variance are shown in Table IV. μ_A and σ_A are 3.28 (mV). μ_A is the value we measure in Fig. 2.5. Consequently, we can derive the mean and variance of ΔV_{th} at different recovery time, as expressed below,

$$\sigma^2=\frac{\sum_{i=1}^{n}x_i^{\,2}}{n}-\mu^2 \qquad \text{Eq. (3.14)}$$

$$\sigma_1^2=\frac{\sum_{i=n_0+1}^{n_0+n_1}x_i^{\,2}}{n_1}-\mu_1^2 \quad\Rightarrow\quad \sum_{i=n_0+1}^{n_0+n_1}x_i^{\,2}=n_1(\sigma_1^2+\mu_1^2) \qquad \text{Eq. (3.15)}$$

$$\sigma_2^2=\frac{\sum_{i=n_0+n_1+1}^{n_0+n_1+n_2}x_i^{\,2}}{n_2}-\mu_2^2 \quad\Rightarrow\quad \sum_{i=n_0+n_1+1}^{n_0+n_1+n_2}x_i^{\,2}=n_2(\sigma_2^2+\mu_2^2) \qquad \text{Eq. (3.16)}$$

And so on.

$$\sigma_{total}^2 = \frac{\sum_{i=1}^{N} x_i^{\,2}}{N} - \mu_{total}^2 = \frac{\sum_{i=n_0}^{n_0+n_1} x_i^{\,2} + \sum_{i=n_0+n_1}^{n_0+n_1+n_2} x_i^{\,2} + \ldots.}{N} - \mu_{total}^2$$

$$= \frac{\mathrm{n}_1(\sigma_1^2+\mu_1^2)+\mathrm{n}_2(\sigma_2^2+\mu_2^2)+\mathrm{n}_3(\sigma_3^2+\mu_3^2)+\ldots}{N} - (P_1\mu_1 + P_2\mu_2 + \ldots + P_{\mathrm{M}}\mu_{\mathrm{M}})^2$$

$$= \sum_{i=1}^{M} P_i(\sigma_i^2+\mu_i^2) - (\sum_{i=1}^{M} P_i\mu_i)^2 \qquad \text{Eq. (3.17)}$$

$$\mu_{total} = P_1\mu_1 + P_2\mu_2 + \ldots + P_M\mu_{\mathrm{M}} = \sum_{i=1}^{M} P_i\mu_i \qquad \text{Eq. (3.18)}$$

where $N = n_0 + n_1 + n_2 + n_3 + \cdots$; $P_i = \frac{n_i}{N}$, i=0,1,2,3...

M is the maximum de-trapping number of our measured devices.

The closed form and Monte Carlo simulation result is shown in Fig. 3.12. The mean and variance of ΔV_{th} fit the results of Monte Carlo simulation very well.

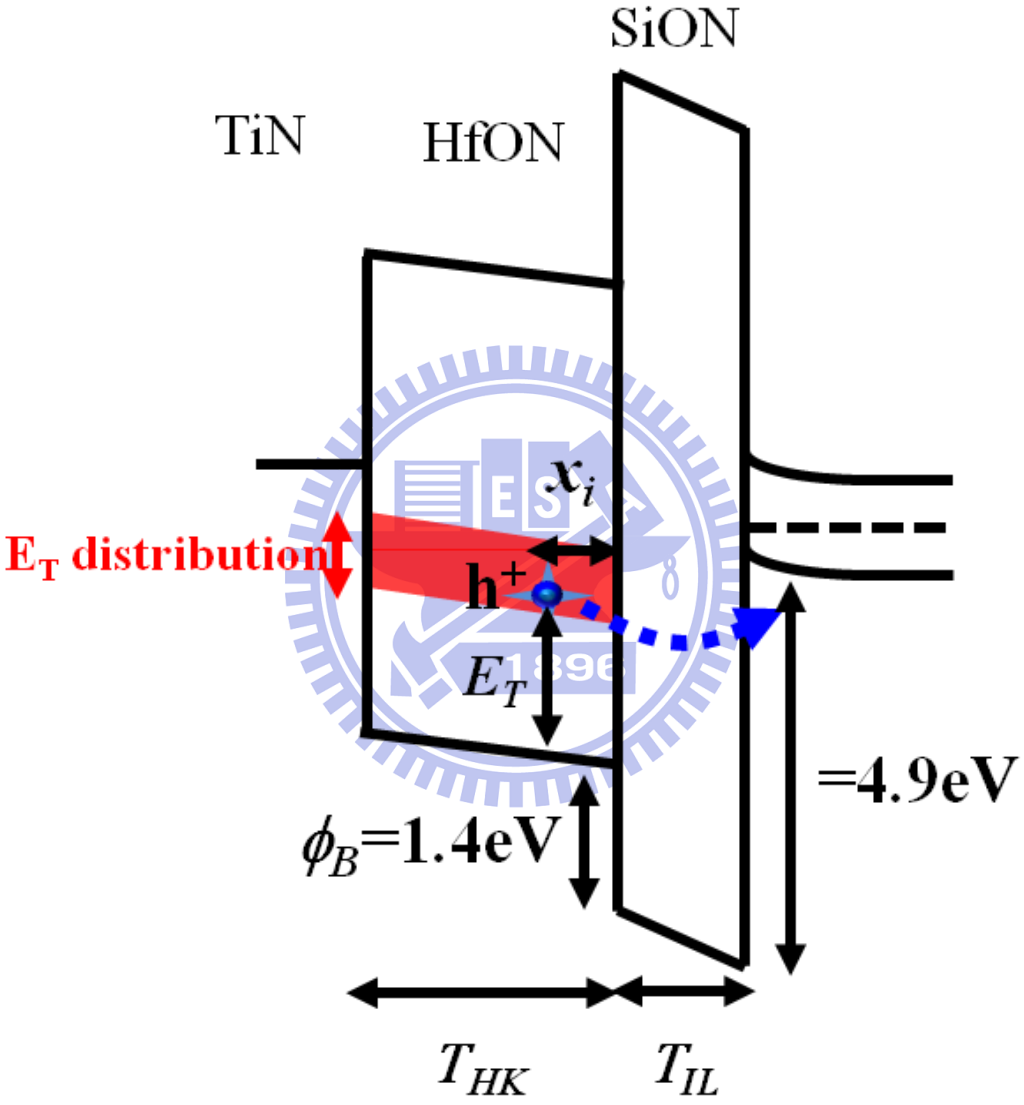

Fig. 3.1 Schematic representation of band diagram and trap positions in recovery phase.

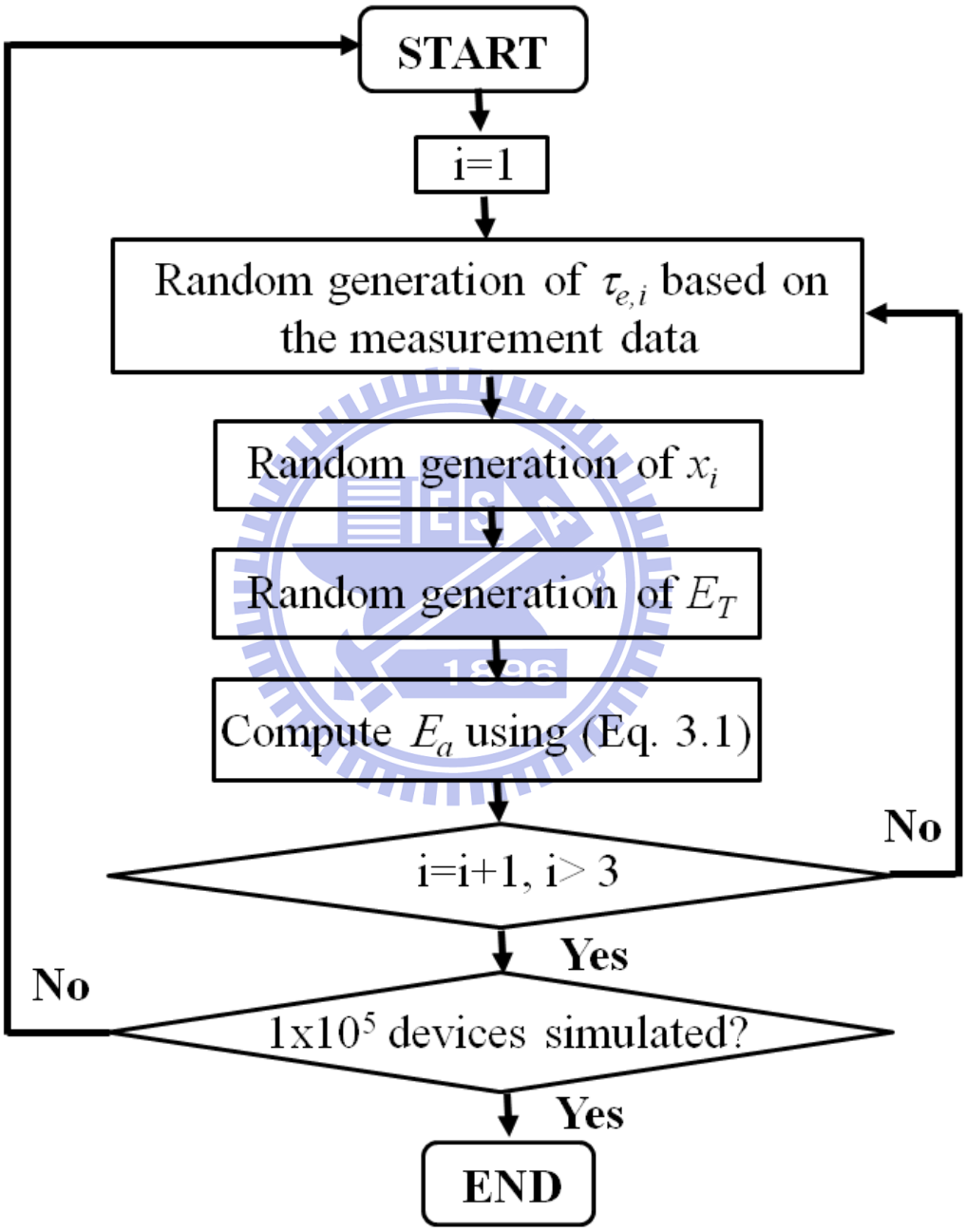

Fig. 3.2 Flow of E_a extraction

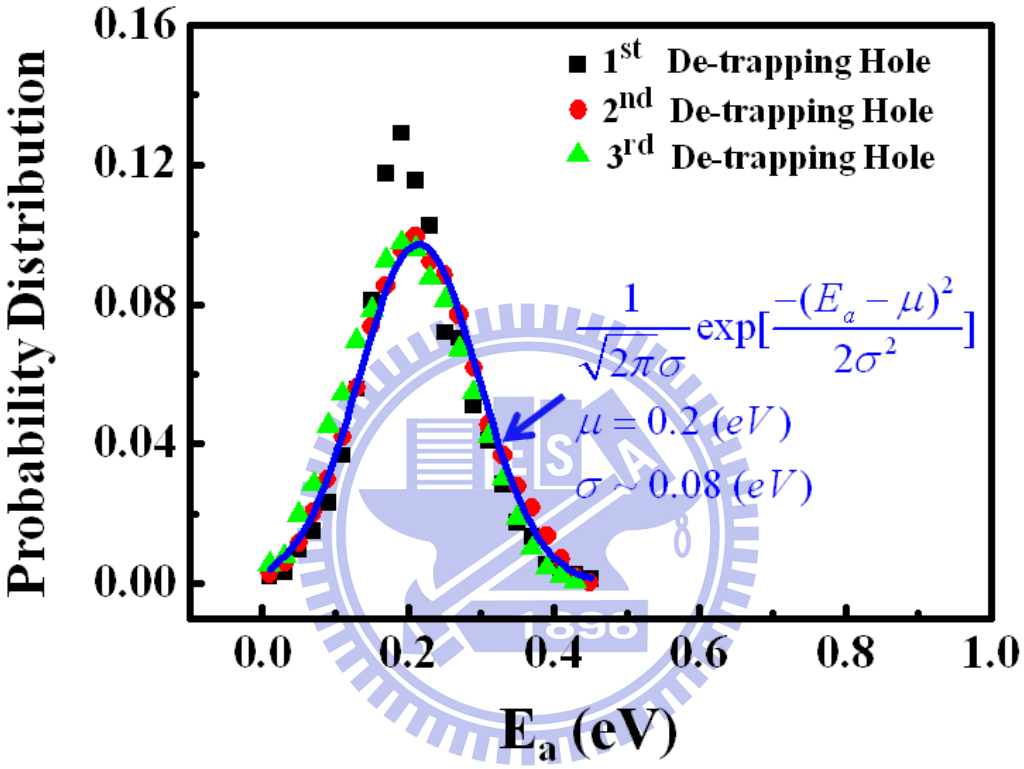

Fig. 3.3 Extracted E_a from $\tau_{e,i}$ Distribution

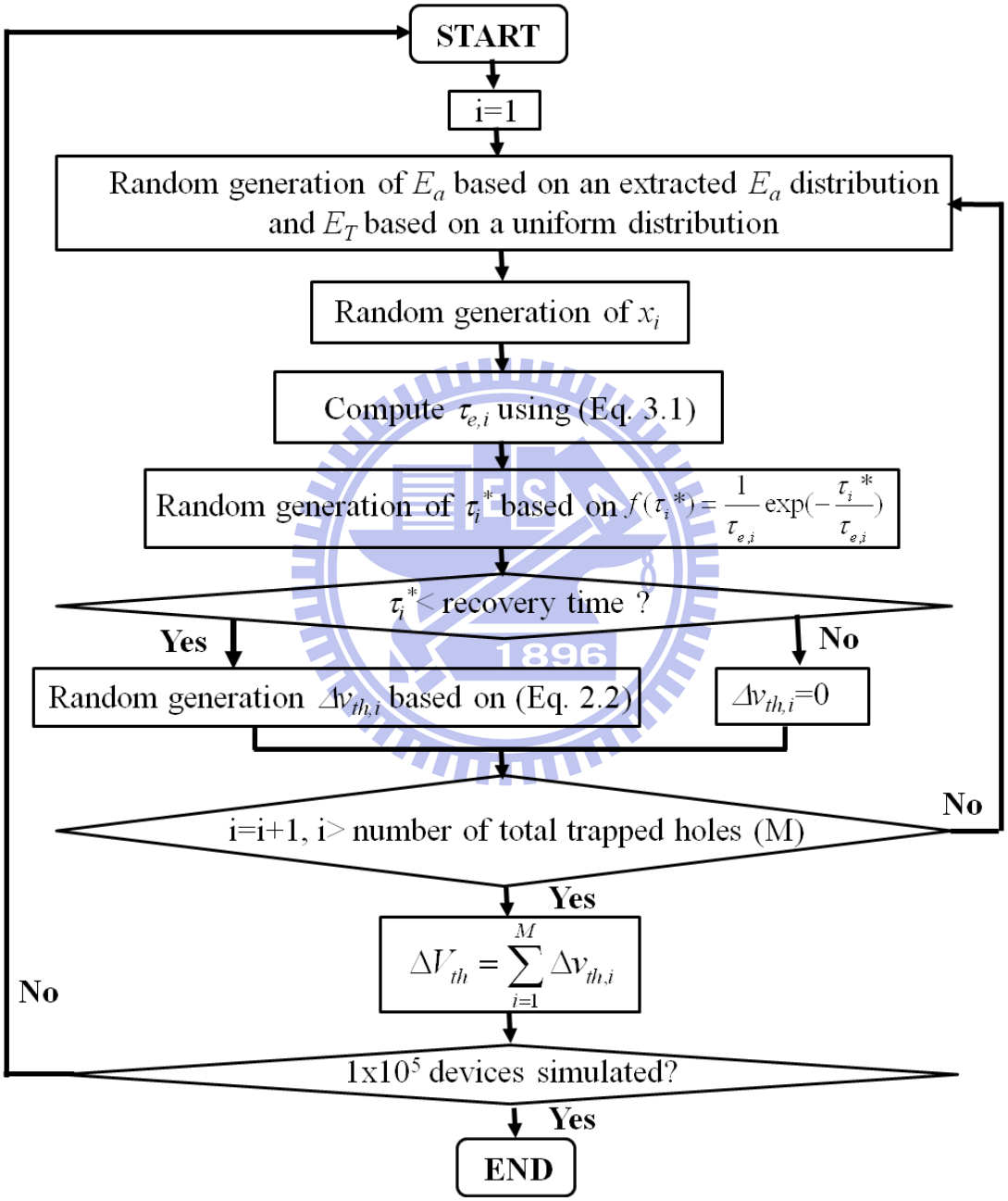

Fig. 3.4 Flow chart of Monte Carlo simulation.

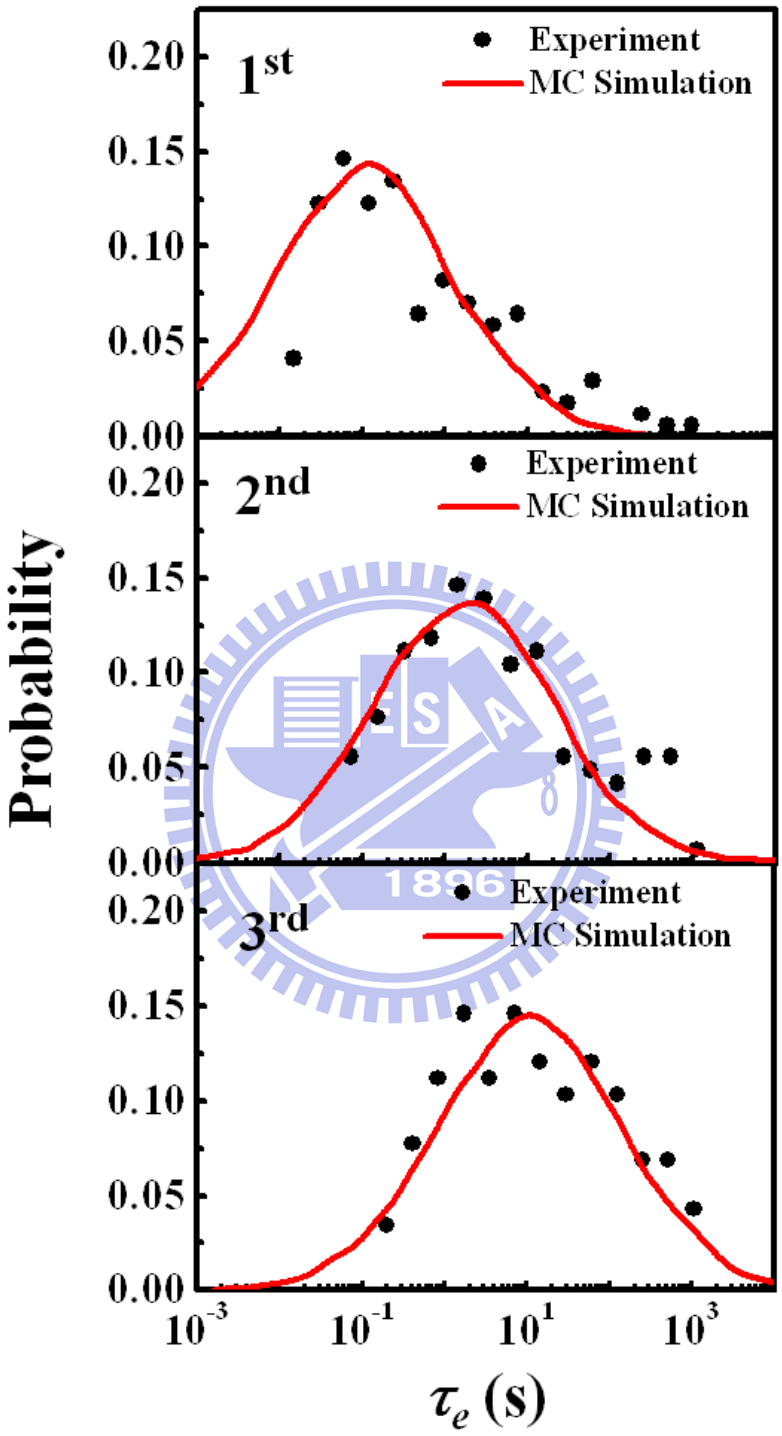

Fig. 3.5 The probability distribution of trapped charge de-trapping time (τ_e) in NBTI recovery. Monte Carlo simulation result fits the measurement data well.

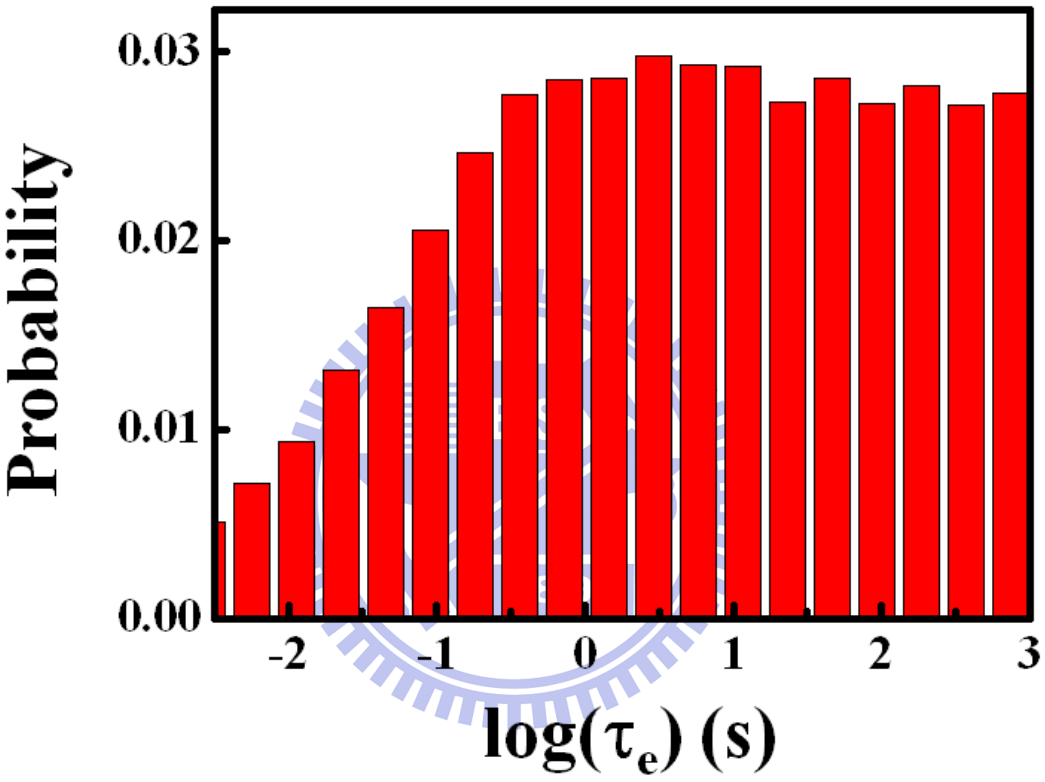

Fig. 3.6 MC simulation result of total τ_e distribution.

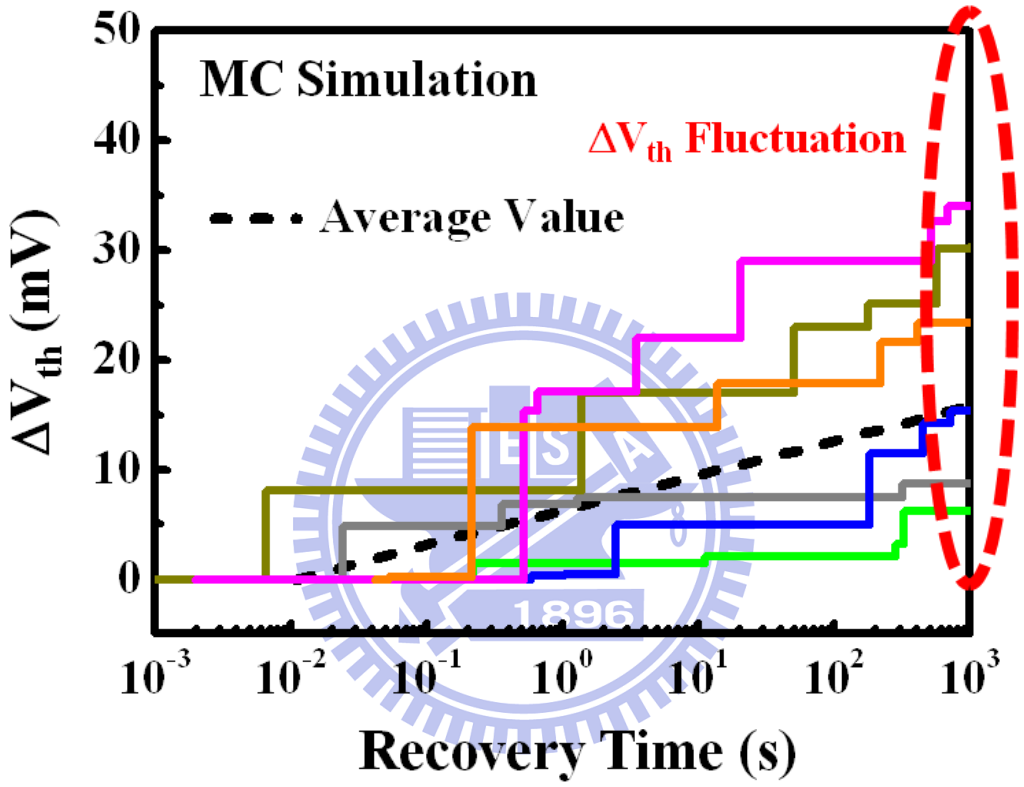

Fig. 3.7 Simulation of stair-like ΔV_{th} fluctuation.

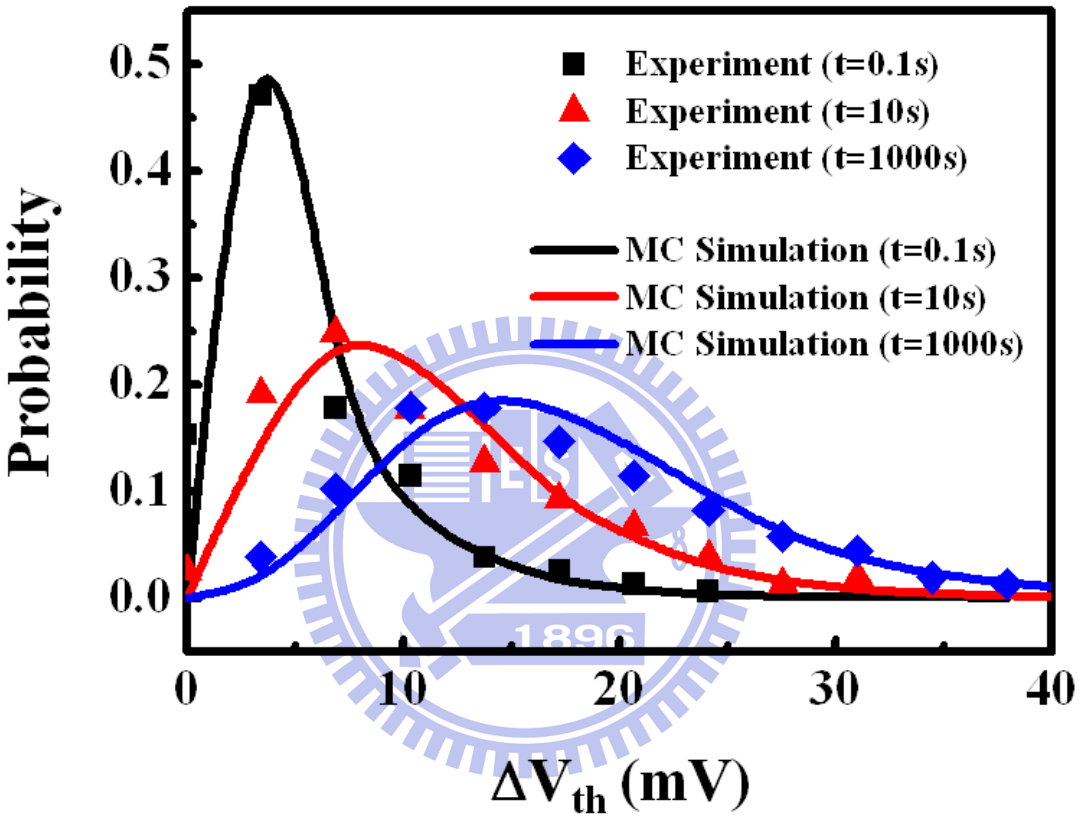

Fig. 3.8 Probability distribution of NBTI recovery induced ΔV_{th} at 0.1s, 10s, and 1000s from measurement and Monte Carlo simulation.

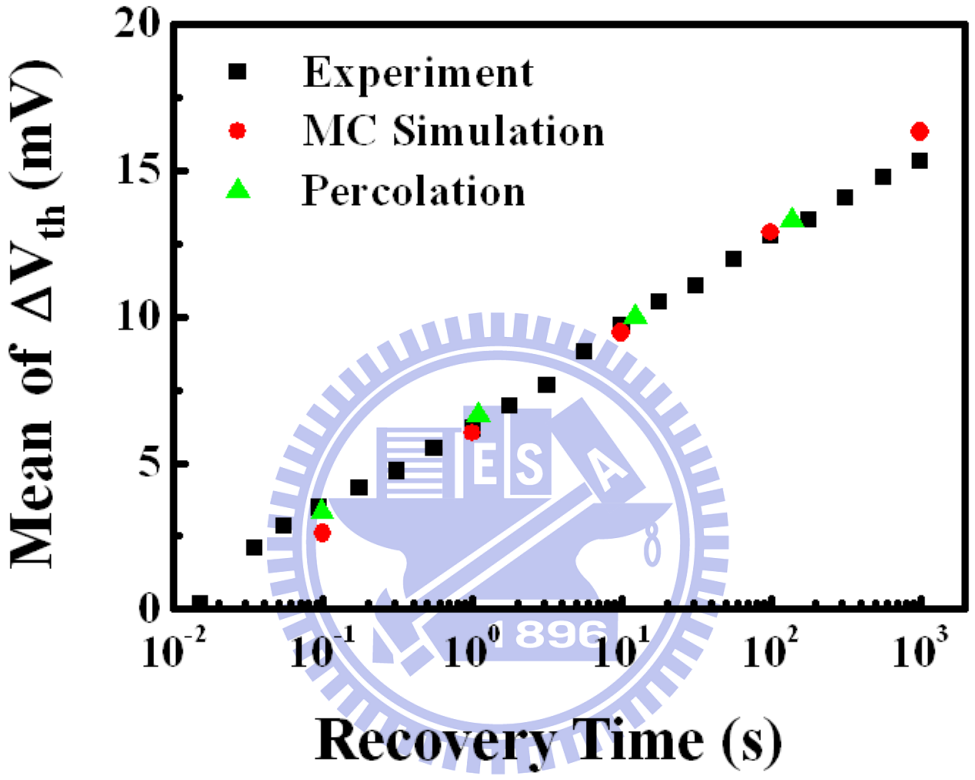

Fig. 3.9 The mean value of the ΔV_{th} distribution versus NBTI recovery time from measurement and Monte Carlo simulation. Percolation has δ-function like E_a and E_T distribution.

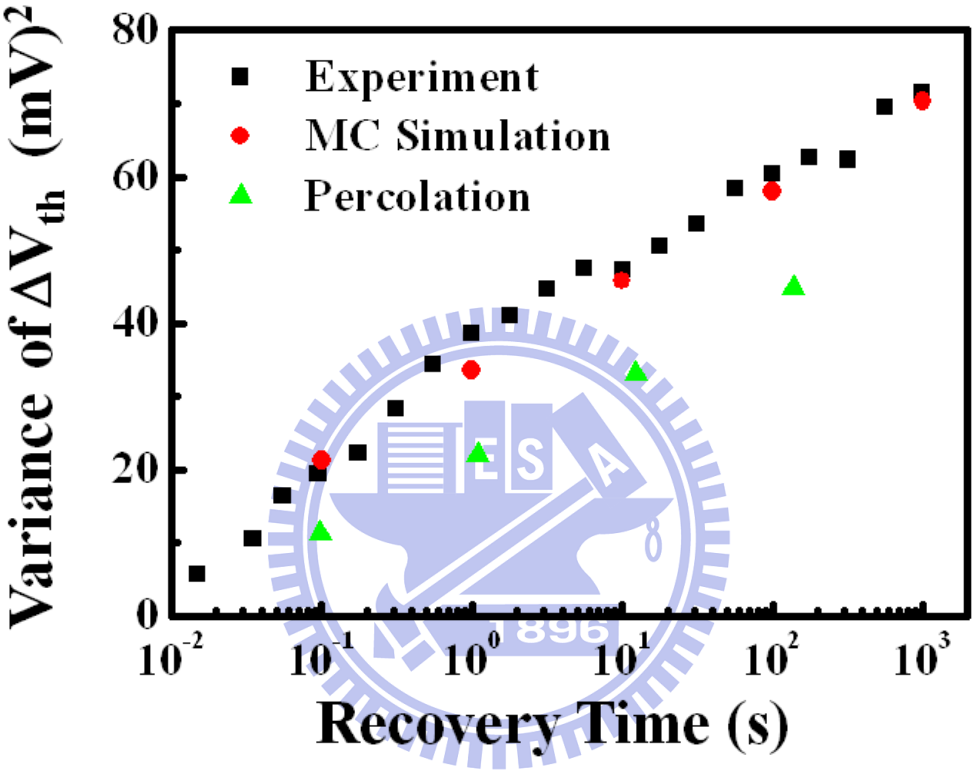

Fig. 3.10 The variance of the ΔV_{th} distribution versus NBTI recovery time from measurement and Monte Carlo simulation. Percolation has δ-function like E_a and E_T distribution.

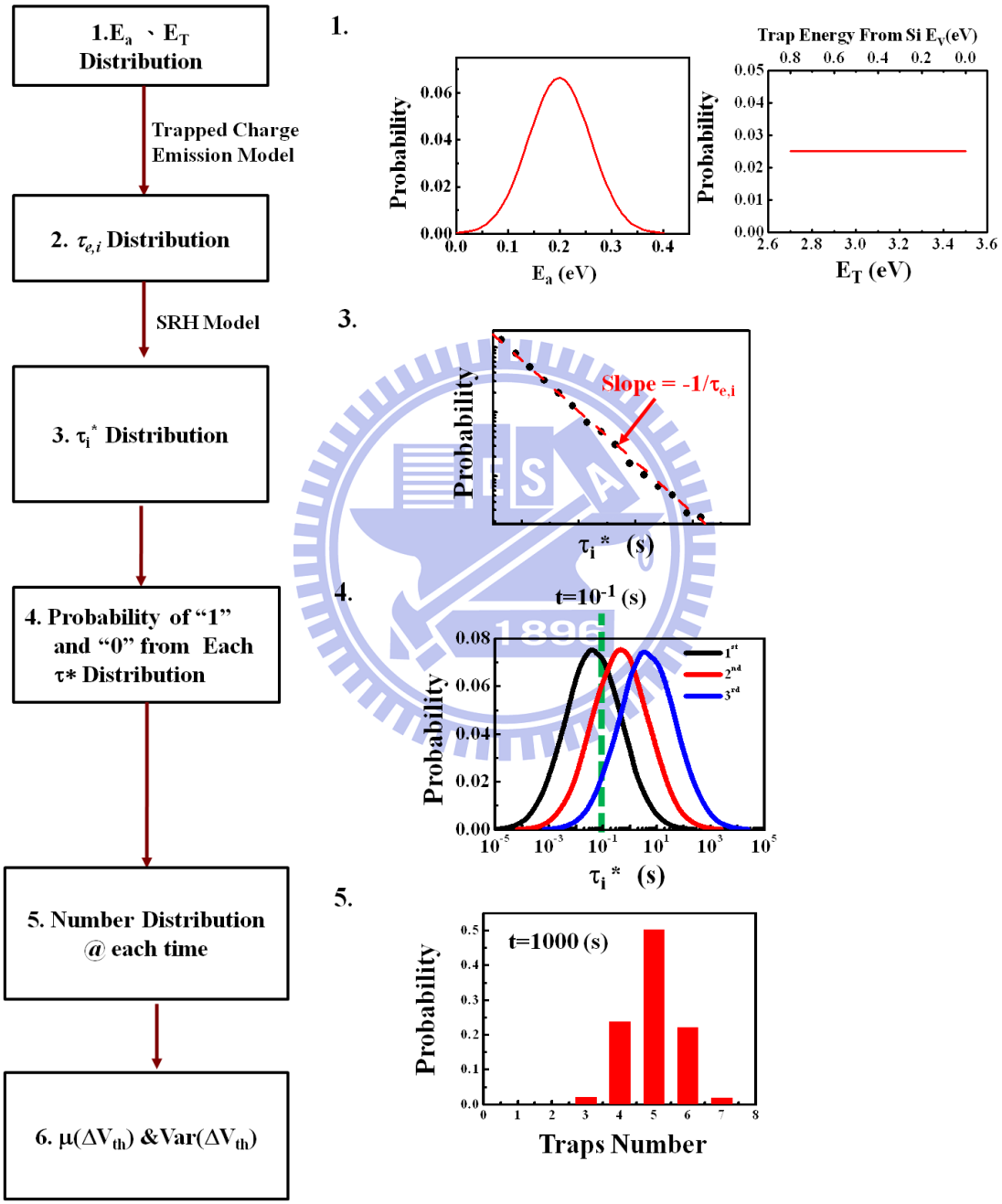

Fig. 3.11 Flow chart of closed form method.

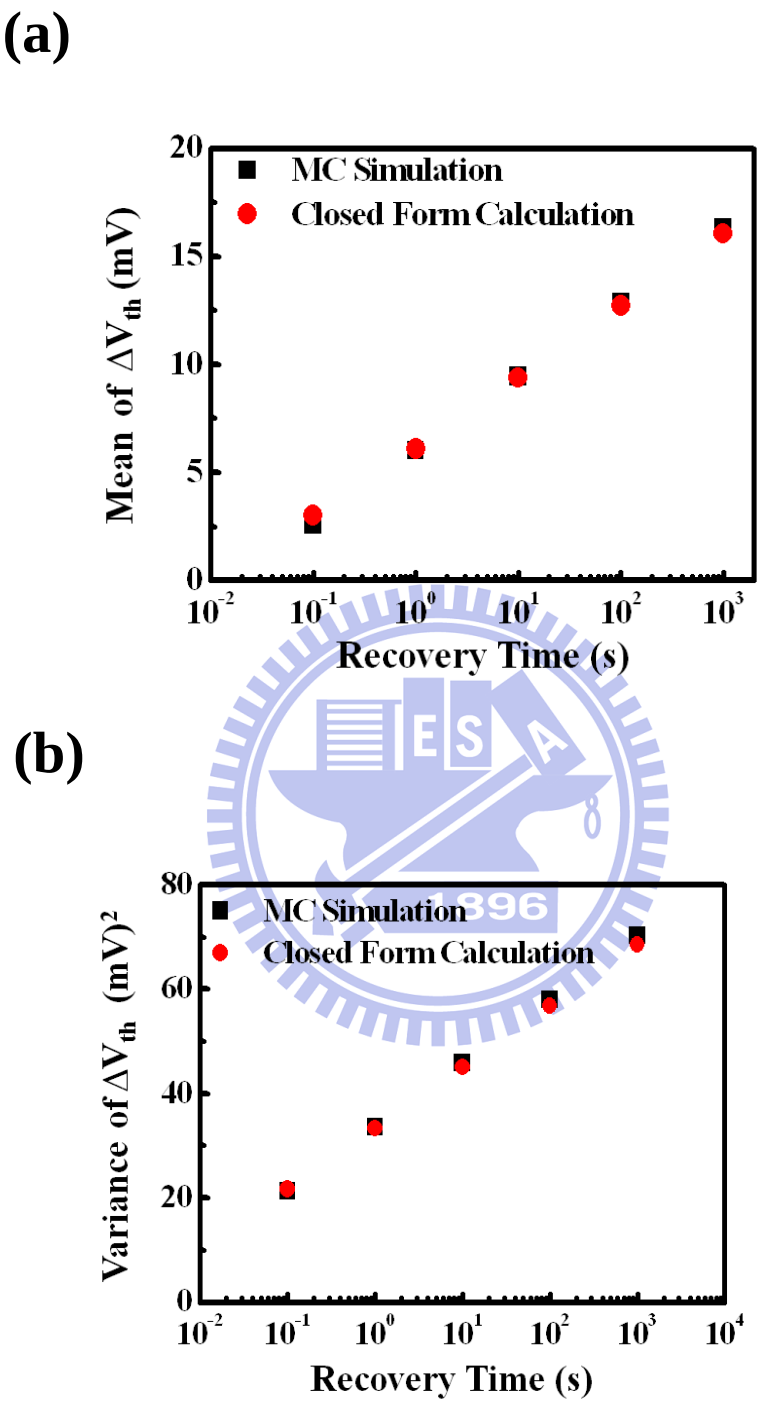

Fig. 3.12 The (a) mean value and (b) variance of the ΔV_{th} distribution versus NBTI recovery time from Monte Carlo simulation and closed form method.

	1st	2nd	3rd
σ of E_a (eV)	0.078	0.084	0.082

Table II σ of extracted E_a from $\tau_{e,1}$, $\tau_{e,2}$, and $\tau_{e,3}$.

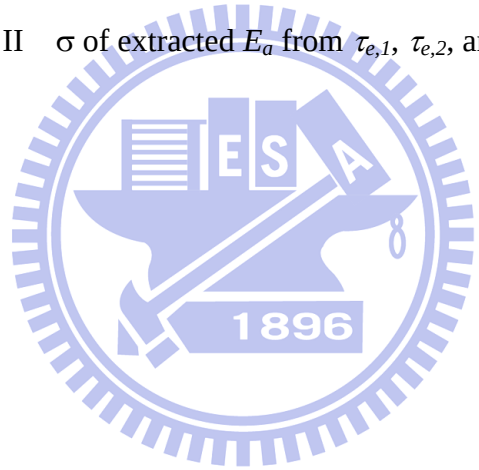

μ_i	i=1	i=2	i=3
Experiment	-1.019	0.036	1.064
MC Simulation	-0.982	0.029	1.035

σ_i	i=1	i=2	i=3
Experiment	1.070	1.181	1.285
MC Simulation	1.098	1.146	1.196

Table III μ and σ of the first three de-trapping time distribution from measurement and Monte Carlo simulation.

Number	1	2	3	.....	M
μ	$\mu_1 = \mu_A$	$\mu_2 = 2\mu_A$	$\mu_3 = 3\mu_A$	.....	$\mu_M = M\mu_A$
σ²	$\sigma_1^2 = \sigma_A^2$	$\sigma_2^2 = 2\sigma_A^2$	$\sigma_3^2 = 3\sigma_A^2$	.....	$\sigma_M^2 = M\sigma_A^2$
Probability	P_1	P_2	P_3	.....	P_M

Table IV μ, σ^2, and probability of each de-trapping hole number.

Chapter 4

Conclusion

Single charge emission from traps in the high-κ gate dielectric is observed in small-size devices. Physics of single charge de-trapping induced ΔV_{th} in NBTI recovery is characterizing in this work. Two factors are found to affect a NBTI ΔV_{th} distribution. One is the dispersion of single charge de-trapping induced Δv_{th}. The other one is the dispersion of de-trapping time. The cumulative probability distribution of Δv_{th} amplitude follows the exponential distribution. The individual de-trapping time has Gaussian-like distribution. The occurrence distribution of total de-trapping time is a uniform distribution, which implies the trap is a uniform distribution in high-κ layer spatially.

From the measured $\tau_{e,i}$ distributions, E_a is extracted using trapped charge emission model. The extracted E_a is a Gaussian-like distribution. According to the Δv_{th} amplitude distribution and the de-trapping time obtained from the experiment, a Monte Carlo simulation employing the trapped charge emission model and taking account the E_a and E_T distributions is developed to simulate a ΔV_{th} distribution and its recovery time evolution. We extract the mean value and the variance of the ΔV_{th} distribution at different recovery times. The mean value of the ΔV_{th} follows a logarithm dependence on recovery time. The ΔV_{th} distribution broadens with an increasing recovery time. Furthermore, we also calculate the mean value and the variance of the ΔV_{th} distribution at different recovery times using closed form method. These two simulation results fit the experimental data well.

Reference

[1] J. Robertson, “Interfaces and defects of high-K oxides on silicon,” *Solid State Electron*, vol. 49, no. 3, pp. 283-293, 2005.

[2] G. D. Wilk, R.M. Wallace, and J. M. Anthony, “High-k gate dielectrics：Current status and materials properties considerations,” *J. Appl. Phys.*, vol. 89, no. 10, pp.5243-5801, 2001.

[3] C.Fobbs, L. Fonseca, V. Dhandapani, S. Samavedam, B. Taylor, J. Grant, L.Dip, D. Triyoso, R. Hegde, D. Gilmer, R.Garcia, D.Roan, L.Lovejoy, R. Rai, L. Hebert, H. Tseng, B. White, and P. Tobin, “Fermi level pinning at the poly-Si/metal oxide interface,” in *VLSI Symp. Tech. Dig*., pp. 9-10, 2003.

[4] S. Zafar, Y.H. Kim, V. Narayanan, C. Cabral Jr., V. Paruchri, B. Doris, J. Stathis, A. Callegari, and M. Chudzik, “A Comparative Study of NBTI and PBTI (Charge Trapping) in SiO2/HfO2 Stacks with FUSI, TiN, Re Gates,” in *VLSI Symp. Tech. Dig*., pp. 23-25, 2006.

[5] V. Reddy, A.T. Krishnan, A. Marshall, J.Rodriguez, S. Natarajan, T. Rost, S. Krishnan, “Impact of negative bias temperature instability on digital circuit reliability,” in *Microelectronics Reliability.*, Vol. 45, pp. 31–38, 2005

[6] M.A. Alam, and S. Mahapatra, “A comprehensive model of PMOS NBTI degradation” in *Microelectronics Reliability.*, pp. 71-81, 2005.

[7] H. Kufluoglu, and M.A. Alam, “A generalized reaction-diffusion model with explicit H–H2 dynamics for negative-bias temperature-instability (NBTI) degradation,” *IEEE Trans. Electron Devices*, vol. 54, no. 5, pp. 1101-1107, 2007.

[8] T. Grasser, B. Kaczer, W. Goes, H. Reisinger, T. Aichinger, P. Hehenberger, P.-J. Wagner, F. Schanovsky, J. Franco, M. Toledano, and M. Nelhiebel, "The Paradigm Shift in Understanding the Bias Temperature Instability：From Reaction-Diffusion to Switching Oxide Traps," *IEEE Trans. Electron Devices*, vol. 58, no. 11, pp. 3652-3665, 2011.

[9] V. Huard, M. Denais, and C. Parthasarathy, "NBTI degradation: from physical mechanism to modeling," in *Microelectronics Reliability.*, Vol. 46, pp. 1–23, 2006

[10] T. Wang, C.T. Chan, C.J. Tang, C.W. Tsai, H.C.-H. Wang, M.H. Chi, and D.D. Tang, "A Novel Transient Characterization Technique to Investigate Trap Properties in HfSiON Gate Dielectric MOSFETs─From Single Electron Emission to PBTI Recovery Transient," *IEEE Trans. Electron Devices*, vol. 53, no. 5, pp. 1073-1079, 2006.

[11] C.T. Chan, H.C. Ma, C.J. Tang, and T. Wang, "Investigation of Post-NBTI Stress Recovery in pMOSFETs by Direct Measurement of Single Oxide Charge De-Trapping," i*n VLSI Symp. Tech. Dig*., pp. 90-91, 2005.

[12] C.T. Chan, C.J. Tang, C.H. Kuo, H.C. Ma, C.W. Tsai, H.C.-H. Wang, M.H. Chi, and T. Wang, "Single-Electron Emission of Traps in HfSiON as High-k Gate Dielectric for MOSFETs," in *Proc. IRPS*, pp.41-44, 2005.

[13] A. Shanware, M.R. Visokay, J.J. Chambers, A.L.P. Rotondaro, H. Bu, M.J. Bevan, R. Khamankar, S. Aur, P.E. Nicollian, J. McPerson, and L, Colombo, "Evaluation of the Positive Biased Temperature Stress Stability in HfSiON Gate Dielectrics," in *Proc. IRPS*, pp.208-213, 2003.

[14] S. Rangan, N. Mielke, and E. C.C. Yeh, “Universal Recovery Behavior of Negative Bias Temperature Instability,” in *IEDM Tech. Dig.*, pp. 341-344, 2003.

[15] A. Asenov, R. Balasubramaniam, A.R. Brown, and J.H. Davies, “RTS Amplitudes in Decananometer MOSFETs：3-D Simulation Study,” *IEEE Trans. Electron Devices*, vol. 50, no. 3, pp. 839-845, 2003.

[16] T. Grasser, B. Kaczer, W. Goes, Th. Aichinger, Ph. Hehenberger, and M. Nelhiebel, “A Two-Stage Model for Negative Bias Temperature Instability,” in *Proc. IRPS*, pp.33-44, 2009.

[17] H.Y. Yu, Y.T. Hou, M.F. Li, and D.-L. Kwong, “Hole Tunneling Current Through Oxynitride/Oxide Stack and the Stack Optimization for p-MOSFETs,” *IEEE Electron Device Lett.*, vol. 23, no. 5, pp. 285-287, 2002.

[18] Y.T. Hou, M.F. Li, H.Y. Yu, Y. Jin, and D.-L. Kwong, “Quantum Tunneling and Scalability of HfO_2 and HfAlO Gate Stacks,” in *IEDM Tech. Dig.*, pp. 731-734, 2002.

簡　　歷

姓名:謝泓達

性別:男

生日:民國 77 年 6 月 8 日

籍貫:台灣省台南縣

地址:台南市佳里區安南路 52 巷 14 號

學歷:國立暨南國際大學 應用材料及光電工程　95.9-99.6

國立交通大學電子工程研究所碩士班　99.9-101.7

碩士論文題目:

在負偏壓溫度不穩定回復時臨界電壓改變量分佈之統計特性和模式及其時間演繹

Statistical Characterization and Modeling of ΔV_{th} Distribution in NBTI Recovery and Its Time Evolution